(MSC100/TM300; Courage +Khazaka electronic GmbH, Köln, Germany).

Assessment of Pain

The pain associated with application of microneedle patches was expressed numerically using a Visual Analogue Scale (VAS) from 0 (no pain) to 100 (unbearable pain).

RESULTS

Comparison of Fundamental Characteristics of New-MH and Old-MH

We investigated dissolution kinetics of microneedles in mice and rats, whose skins differ in hardness and in thickness by approximately 10 μm. New-MH200 and new-MH300 microneedle

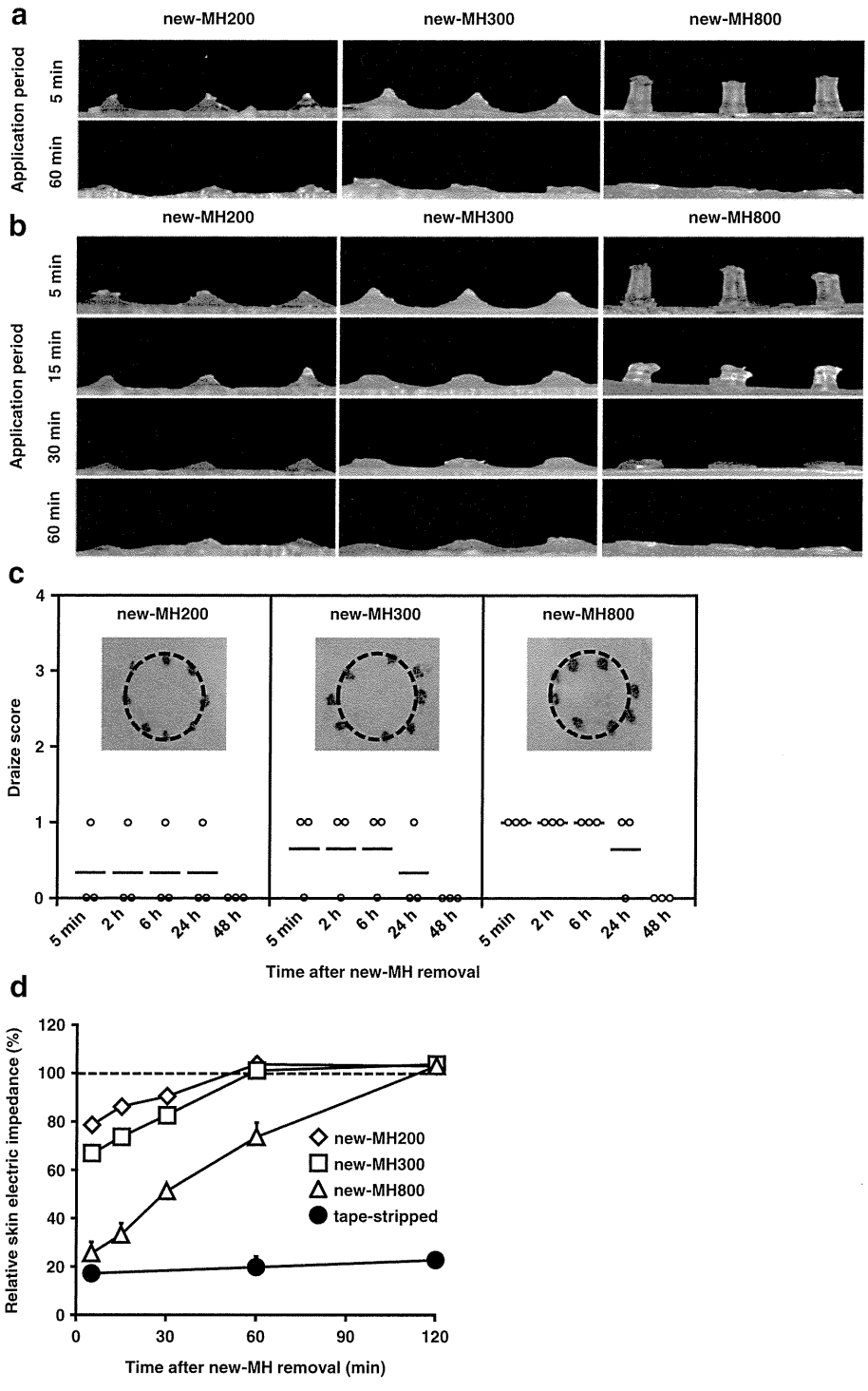

Fig. 2 Needle-dissolution kinetics of new-MH, and skin status after application of new-MH. (**a** and **b**) New-MH200, new-MH300, and new-MH800 were applied on the back skin of BALB/c mice (**a**) or Wistar ST rats (**b**) for the indicated times. After removal of new-MH, the microneedles remaining on each new-MH were photographed using a stereoscopic microscope. (**c**) New-MH200, new-MH300, or new-MH800 were applied to the back skin of Wistar ST rats for 30 min. The degree of erythema on the skin of Wistar ST rats was scored using the Draize scoring system: 0, no erythema or edema; 1, very slight erythema and/or barely perceptible edema; 2, well-defined erythema and/or slight edema; 3, moderate to severe erythema or moderate edema, and 4, severe erythema and/or edema, 5 min, 2 h, 6 h, 24 h, or 48 h after removing new-MHs. The mean score is shown as a bar. Each panel shows photographs of application areas 5 min after new-MH removal. (**d**) Skin impedance of new-MH application areas and non-application areas was measured 5, 15, 30, 60, and 120 min after 30-min applications. As controls, back skin of Wistar ST rats were tape-stripped. Data are expressed as mean ± SE of data from three rats.

tips dissolved rapidly and microneedles on new-MH800 resulted in a 50% reduction in length after 5 min in both mice and rats (Fig. 2a and b). The dissolution of microneedles progressed with application time, and all new-MH had dissolved completely after 60 min. These dissolution kinetics and technique for the insertion of microneedles were identical to those of old-MHs independent of the components. We evaluated erythema and edema at the application site using the Draize scoring system 30 min after applying new-MHs. Five minutes after patch removal, slight erythema was observed in 1 of 3 rats treated with new-MH200, in 2 of 3 rats treated with new-MH300, and in all rats treated with new-MH800. These

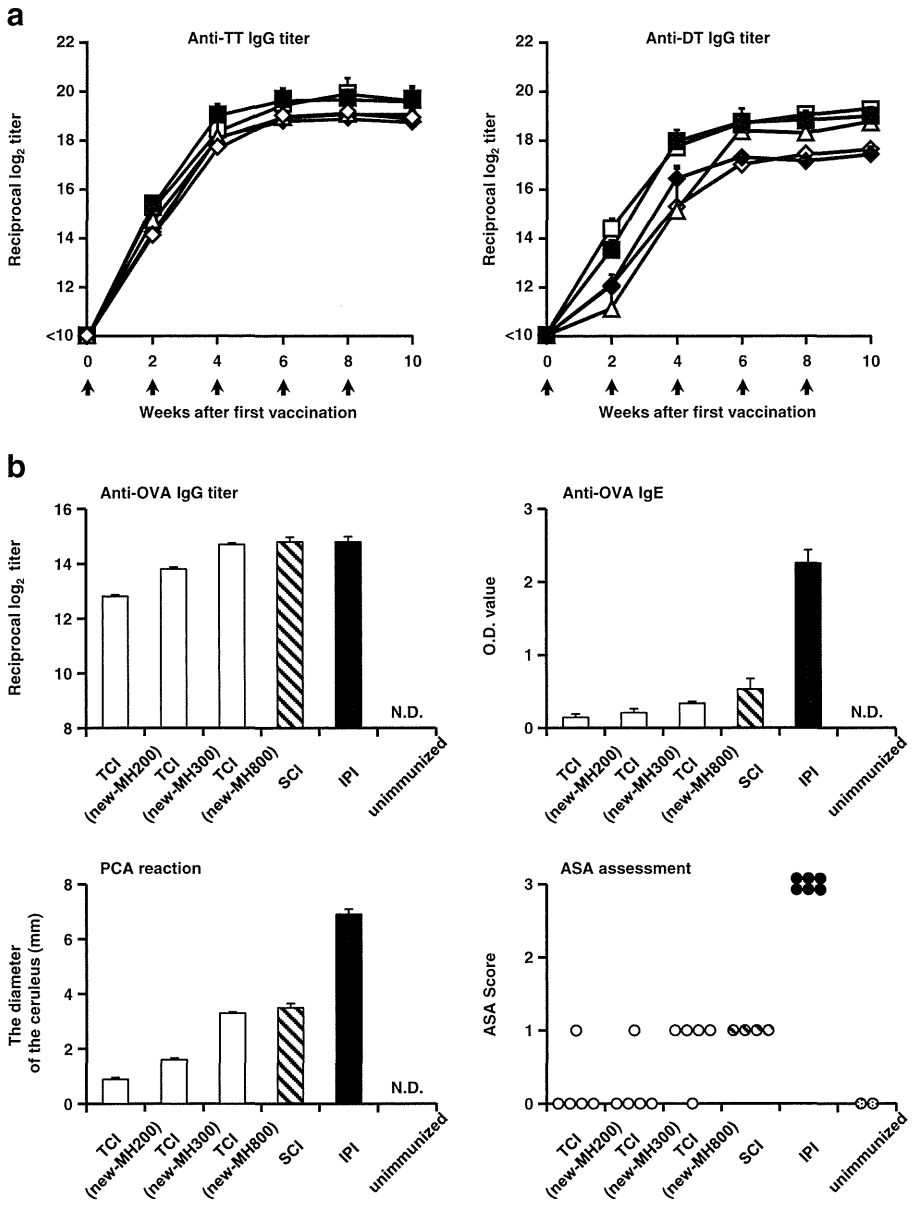

Fig. 3 Immune responses induced by antigen loaded new-MH formulations. (**a**) The new-MH800 (◇ and ♦) or old-MH800 (□ and ■) with 20 μg TT and 10 μg DT/needles were applied to the back skin of Wistar ST rats five times at 2-week intervals for 1 h (◇ and □) or 6 h (♦ and ■). Wistar ST rats were subcutaneously injected with equivalent TT and DT doses (△). At the indicated points, sera collected from these rats were assayed for TT or DT IgG titers by ELISA. Data are expressed as mean ± SE of results from five rats. *Arrows* indicate the vaccination point. (**b**) Hartley guinea pigs were treated with new-MH200, new-MH300, or new-MH800 containing 1 μg OVA/needles for 6 h four times at 2-week intervals, or were subcutaneously immunized with 1 μg OVA (SCI) five times at 2-week intervals. As positive controls, Hartley guinea pigs were immunized by intraperitoneal injection of 1-μg OVA and 5-mg Alum (IPI) twice at 2-week intervals. Two weeks after the final vaccination, sera were collected from these animals and were assayed for OVA-specific IgG titers, and O.D. value of IgE (16-fold dilution) by ELISA. For the PCA reaction, non-sensitized Wistar ST rats were injected with sera from immunized-guinea pigs. Twenty-four hours later, these rats were intravenously injected with Evans blue and OVA, and a leak blue spot at the injection site was measured 30 min later. Data are expressed as mean ± SE of results from 4 to 6 guinea pigs. In ASA assessments, guinea pigs were intravenously injected with OVA a month after the final vaccination, and the performance status of guinea pigs was scored using the ASA scoring system. *N.D.*; not detected.

observations suggest that erythema is exacerbated by needle length (Fig. 2c). However, erythema disappeared within 48 h, and edema was not observed in any rats. Thus, application of new-MH caused only minor irritation of the skin. Using skin impedance measurements, we observed the recovery of skin with microneedle puncture holes. Application of either new-MH200 or new-MH300 decreased skin impedance to 60–80%, whereas application of new-MH800 or tape-strips decreased skin impedance to 20% (Fig. 2d). The impedance of tape-stripped skin did not recover within 120 min. On the other hand, skin impedance recovered within 60 min after removal of new-MH200 or new-MH300 patches, and within 120 min after removal of new-MH800 patches. Therefore, puncture holes that were caused by insertion of microneedles closed within a few hours of new-MH application, indicating a low risk of secondary infection. Given similar fundamental characteristics of new-MH and old-MH, we conclude that new-MH is a safe and minimally invasive device.

Immune Responses Induced by TCI Using Antigen-Loaded New-MH

We selected MH800, and compared vaccine delivery efficiency between TCI using new-MH and old-MH over 1 h or 6 h. The profile of anti-toxoid IgG antibody production following application of new-MH was similar to that of old-MH (Fig. 3a). Thus, we confirmed that the components of microneedles did not influence the intended immune response. In addition, there was no significant difference between the 1-h and 6-h application periods, indicating that the complete dissolution of microneedles within 1 h of application was sufficient to deliver antigen into the skin and to achieve effective vaccination. To further assess vaccination efficacy, we evaluated whether toxoid-specific antibodies, produced by application of new-MH, neutralized tetanus toxin. Immunized rats were resistant to the lethal toxin after tetanus toxin challenge, whereas the rats treated with antigen-free new-MH800 died (Table I). Therefore, we have confirmed that antigen-contained new-MH patches induce a protective immune response against infectious diseases as effectively as those of old-MH (21).

To assess unintended immune responses, we evaluated antigen-specific IgE production in guinea pigs, which is mainly used to identify allergic reactions. Anti-OVA IgG titer increased in all immunized guinea pigs, and the TCI and SCI groups showed little induction of anti-OVA IgE (Fig. 3b). In addition, we conducted PCA and ASA analyses to assess allergic reactions. In the PCA analysis, antigen-specific Evans blue leak from the injection site was measured in sera from immunized guinea pigs. In the IPI group, a positive PCA reaction (>5 mm) was observed; the diameter of the ceruleus was 6.9 mm in a 1/128 dilution of sera. On the other hand, sera of TCI and SCI groups did not give positive PCA reactions, even in undiluted sera. In ASA assessments, allergic reactions, which appeared after injection of antigen into immunized guinea pigs, was evaluated. Positive control guinea pigs died immediately, but guinea pigs of the TCI and SCI groups remained alive. The ASA scores of TCI and SCI groups were all below 1, although minor anaphylactic symptoms were observed in TCI-treated animals following application of new-MH800, as well as in SCI animals. Because these results showed that TCI using new-MH induced antigen-specific immune responses and did not cause allergic reactions, we conclude that new-MH is a safe and efficacious device for practical use in TCI system.

State of the Human Skin After Application of New-MHs

In animal experiments, we showed that the new-MH device is practical and suitable for TCI. Subsequently, we conducted a clinical study to demonstrate the application of new-MHs to human skin. We examined skin using a confocal laser-scanning microscope immediately after 5-s application of new-MH500 or new-MH800 to the human skin. Puncture holes were distinct on the skin surface, and the delivery depth was at least 100 μm (Fig. 4a). As the thickness of human stratum corneum is approximately 10–20 μm, this indicates that the microneedles of new-MH were able to deliver antigen into the epidermal layer of the human skin. Given that the thickness and water content of skin differs between animals and humans, we confirmed the solubility of microneedles in humans at various times after application. After 1 h, the microneedles had completely dissolved in 2 of 3 subjects, and their length was reduced by 50% in the other subject (Fig. 4b). In all subjects, the microneedles fully dissolved within 6 h after new-MH application, although complete dissolution times varied between individuals. These data showed that the new-MH patches deliver antigen to humans in 6 h. Next, we monitored the closing of puncture holes by measuring TEWL as an index of skin barrier

Table I Passive-Challenge Experiment of Wistar ST Rat with Tetanus Toxin

Vaccination			No. of survival rats/ No. of tested rats
Route	Tetanus toxoid (μg/site)	Application period (h)	
TCI; (new-MH800)	20	1	3/3
TCI; (new-MH800)	20	6	5/5
TCI; (old-MH800)	20	1	3/3
TCI; (old-MH800)	20	6	5/5
TCI; (new-MH800)	–	6	0/3
SCI	20	–	3/3

MH MicroHyala; *TCI* transcutaneous immunization; *SCI* subcutaneous immunization

dysfunction. TEWL of treated skin increased immediately after new-MH800 patches were removed and decreased gradually with time (Fig. 4c), indicating rapid recovery of skin barrier function. After 6-h application of new-MH patches, TEWL was lower than that after 5-s or 1-h application. In addition, confocal laser-scanning microscopy showed that the puncture holes tended to close with longer new-MH application periods (Supplementary Material Fig. S1). Hence, given the dissolution kinetics, we did not consider barrier dysfunction or the risk of secondary infection after 6 h applications of new-MH.

To further assess the safety and utility of new-MH patches, we evaluated the pain of new-MH application using VAS assessments in 17 subjects. Among subjects treated with new-MH-needleless, new-MH300, new-MH500, and new-MH800, no significant differences in VAS scores were identified by the Steel–Dwass test (Fig. 4d). We assumed that the VAS scores associated with new-MH-needleless, which did not have microneedles, resulted from the impact of the handheld spring-type applicator. The VAS scores for each new-MH were low, suggesting that the insertion of microneedles into the skin was minimally painful.

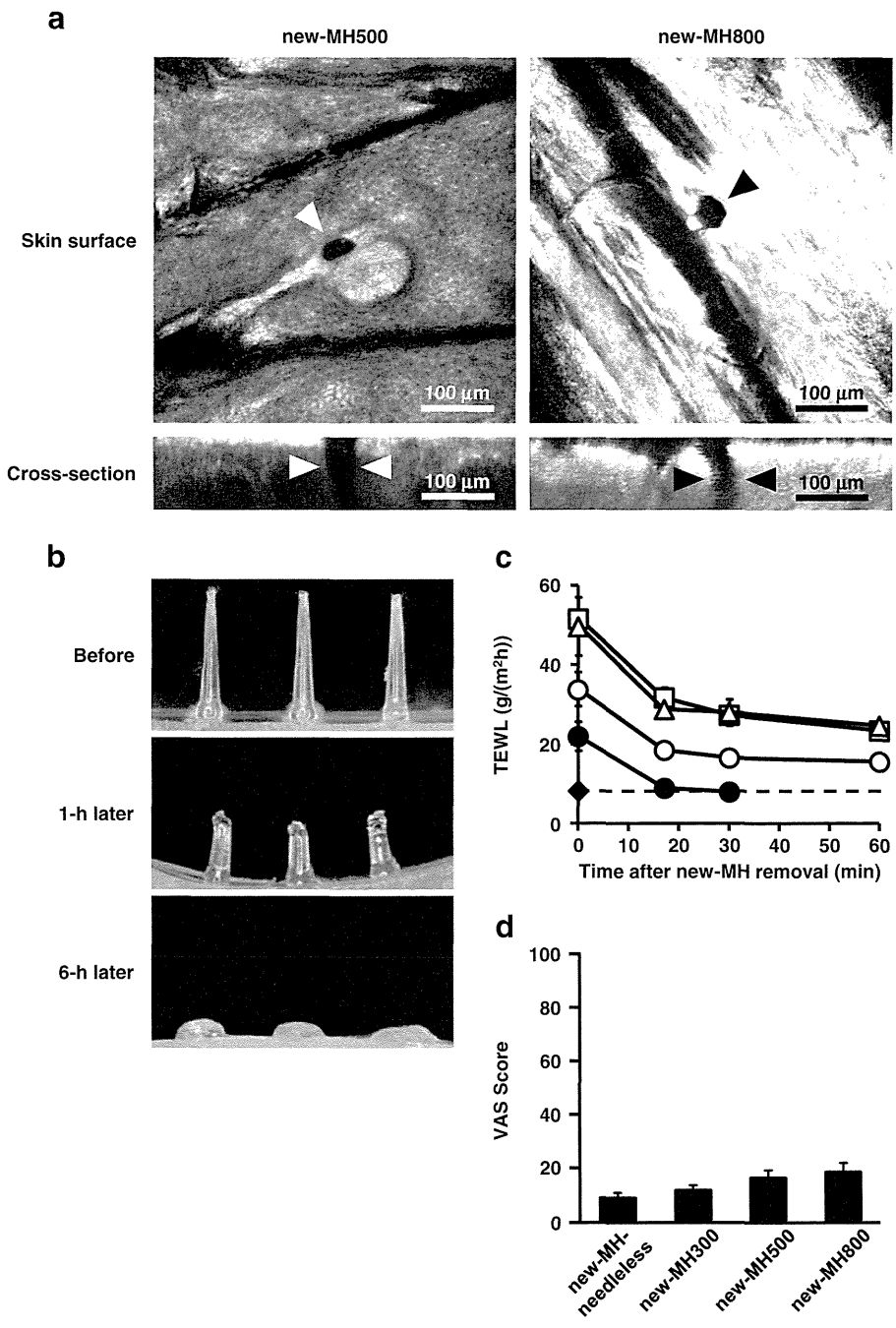

Fig. 4 Status of skin treated with new-MHs, and needle-dissolution of new-MH in humans. (**a**) New-MH800 or new-MH500 were applied to the skin of the left lateral upper arms of two healthy volunteers for 5 s, and skin images were immediately photographed using *in vivo* confocal scanning laser microscopy. (**b**) New-MH800 was applied to the skin of the left lateral upper arms of three healthy volunteers for 1 h or 6 h, and microneedle patches were immediately observed using a stereoscopic microscope. (**c**) New-MH800 was applied to the skin of the left lateral upper arms of three healthy volunteers for 5 s (□), 1 h (△), or 6 h (○). As a control, new-MH-needleless was applied for 6 h (●). At the indicated time after new-MH removal, TEWL of the application sites was measured. Data are expressed as mean ± SE of results from three subjects. ♦; TEWL of untreated skin. (**d**) New-MH-needleless, new-MH300, new-MH500, and new-MH800 were applied to the skin of left lateral upper arms of 17 healthy volunteers. Subjects were asked to grade the pain experienced using a VAS from 0 (no pain) to 100 (unbearable pain). Data are expressed as mean ± SE of results from 17 subjects.

Finally, we assessed local and systemic adverse effects of new-MH application for 6 h in humans. Two days after each new-MH application, faint erythema was observed in 1 subject treated with new-MH300, 12 subjects treated with new-MH500, and 13 subjects treated with new-MH800 (Table II). However, these local responses disappeared in most subjects within 7 days, and skin condition recovered in all subjects within 30 days after application. After application of new-MH500 and new-MH800, purpura, which is caused by capillary damage, was observed in about a half of the subjects. These symptoms disappeared within 30 days, except in the case of one subject with remaining pigmentation that was clinically unproblematic. Application of new-MHs did not cause any systemic adverse effects as determined by a general peripheral blood test and biochemical tests of liver and renal function (Supplementary Material Fig. S2). Thus, we have demonstrated that TCI using new-MH can be applied to humans without severe local or systemic adverse responses.

DISCUSSION

In this study, we prepared new-MH without collagen and investigated the safety of new-MH application to the human skin. We previously reported that old-MH, which contained collagen, is a safe and efficacious device in animal experiments (20,21). However, collagen is suspected to cause allergies in humans. The microneedles of new-MH were inserted into animal skin, and dissolved completely within 1 h as did old-MH. Severe local responses were not observed after application of new-MH. Skin impedance decreased immediately after new-MH application and recovered within 120 min, indicating that the puncture holes caused by new-MH application close rapidly. In addition, we verified that new-MH containing TT and DT induced immune responses that were equal to those produced by old-MH and subcutaneous immunization. Thus, we demonstrated safe application of new-MH to animal skin, effective delivery of the antigen into the skin, and induction of antigen-specific antibodies.

Some researchers have indicated that TCI is more effective than conventional subcutaneous or intramuscular injections (29,30), and in particular, strongly induces Th2 responses (31,32). Because the production of IgE antibody was apprehended during induction of the immune response, we conducted an allergy test of new-MH using guinea pigs. Application of new-MHs did not significantly increase IgE antibodies, and induced an antigen-specific anaphylactic reaction, indicating that new-MH did not induce allergic responses. Thus, we hypothesized that new-MH could be applied to the human skin safely.

Based on these results, we conducted a clinical study of new-MH on the human skin. The microneedles on new-MH successfully penetrated the human skin, which differs in thickness and water content to animal skin, and dissolved completely within 6 h. In animal experiments, we confirmed that there were no significant differences in immune responses between 1-h and 6-h applications of new-MH. Because the application period, in which complete dissolution occurs, may effect induction of the intended immune response, we confirmed that the microneedles of new-MH delivered sufficient antigen into the skin, and induced an immune response in 6 h. Moreover, in TEWL assessments of skin barrier function, skin treated with new-MH for 6 h was more functional than the skin treated for 1 h. Therefore, we decided that 6 h application is necessary to maximize efficacy of antigen delivery and recovery of skin barrier function.

Subsequently, we assessed local and systemic adversities of new-MH application for 6 h in 20 human subjects. Although

Table II Local Adverse Event After Application of New-MHs

new-MH	Day	ICDRG score			Purpura
		−	?+	+	
new-MH300	2	19/20 (95%)	1/20 (5%)	0/20 (0%)	0/17 (0%)
	3	20/20 (100%)	0/20 (0%)	0/20 (0%)	0/17 (0%)
	7	20/20 (100%)	0/20 (0%)	0/20 (0%)	0/17 (0%)
	30	20/20 (100%)	0/20 (0%)	0/20 (0%)	0/17 (0%)
new-MH500	2	8/20 (40%)	12/20 (60%)	0/20 (0%)	6/17 (35.3%)
	3	13/20 (65%)	6/20 (30%)	1/20 (5%)	8/17 (47.1%)
	7	19/20 (95%)	0/20 (0%)	1/20 (5%)	6/17 (35.3%)
	30	20/20 (100%)	0/20 (0%)	0/20 (0%)	0/17 (0%)
new-MH800	2	7/20 (35%)	13/20 (65%)	0/20 (0%)	6/17 (35.3%)
	3	13/20 (65%)	7/20 (35%)	0/20 (0%)	10/17 (58.8%)
	7	19/20 (95%)	1/20 (5%)	0/20 (0%)	5/17 (29.4%)
	30	20/20 (100%)	0/20 (0%)	0/20 (0%)	0/17 (0%)

International Contact Dermatitis Research Group (ICDRG)

−, negative reaction; ?+, doubtful reaction, faint erythema only; +, weak (non-vesicular) positive reaction, erythema, infiltration and possibly papules

application of new-MH caused slight erythema in a few subjects, most reactions disappeared within 30 days. In addition, severe systemic adverse events were not observed in blood tests. Thus, we have shown that this new-MH device can be safely applied to the human skin.

In recent years, Intanza/IDflu (Sanofi Pasteur) has been approved as a novel method for influenza vaccination. Intanza/IDflu uses a "Soluvia" (Becton Dickinson) device, which has a single 1.5-mm long needle that allows intradermal injection of vaccine. While Intanza/IDflu has proven skin targeting vaccination efficacy, the use of needles that are longer than 1 mm has the disadvantage of pain. Therefore, the development of a painless vaccination system using microneedles of less than 1-mm length is required. In previous studies, various microneedles such as hollow microneedles and coating microneedles, have been developed (16,33). However, the hollow needle formulation requires cold chain storage and transportation of antigen solutions, and the coating microneedle formulation is limited by the quantity of antigen that can be coated onto microneedle surfaces. To date, these microneedle technologies have not become practical to use. Our new-MH has the potential to overcome these problems, because antigen is contained within the microneedles. Indeed, the present data greatly contribute to the practical use of microneedle devices, and we are performing clinical studies to assess safety and efficacy of new-MH in the delivery of seasonal trivalent influenza HA antigens. Furthermore, applicators for self-administration are being developed for microneedle formulations.

CONCLUSIONS

We prepared collagen-free new-MH for clinical use, and confirmed that there were no differences in safety and efficacy between new-MH and old-MH. In addition, this study shows that new-MH is safely applicable to the human skin. We expect that this innovative new-MH TCI system for vaccine delivery will greatly decrease the mortality and morbidity that is associated with preventable infectious diseases.

ACKNOWLEDGMENTS AND DISCLOSURES

We are grateful to The Research Foundation for Microbial Diseases of Osaka University (Suita, Japan) for providing tetanus and diphtheria toxoids. This work was supported by the Advanced research for medical products Mining Program of the National Institute of Biomedical Innovation (NIBIO), by Health and Labour Sciences Research Grants in Research on New Drug Development from the Ministry of Health, Labour and Welfare, and by a Grant-in-Aid for Scientific Research (B) (24390041) from the Ministry of Education, Culture, Sports, Science, and Technology of Japan. The authors would like to thank Enago (www.enago.jp) for the English language review.

REFERENCES

1. Azad N, Rojanasakul Y. Vaccine delivery-current trends and future. Curr Drug Deliv. 2006;3(2):137–46.
2. Kersten G, Hirschberg H. Needle-free vaccine delivery. Expert Opin Drug Deliv. 2007;4(5):459–74.
3. UNICEF's work on immunisation. http://www.unicef.org.uk/UNICEFs-Work/What-we-do/UNICEFs-work-on-immunisation/
4. Leppin A, Aro AR. Risk perceptions related to SARS and avian influenza: theoretical foundations of current empirical research. Int J Behav Med. 2009;16(1):7–29.
5. Haque A, Lucas B, Hober D. Influenza A/H5N1 virus outbreaks and prepardness to avert flu pandemic]. Ann Biol Clin. 2007;65(2):125–33.
6. Valadas E, Antunes F. Tuberculosis, a re-emergent disease. Eur J Radiol. 2005;55(2):154–7.
7. Campbell CC. Malaria: an emerging and re-emerging global plague. FEMS Immunol Med Microbiol. 1997;18(4):325–31.
8. Glenn GM, Scharton-Kersten T, Alving CR. Advances in vaccine delivery: transcutaneous immunisation. Expert Opin Investig Drugs. 1999;8(6):797–805.
9. Levine MM. Can needle-free administration of vaccines become the norm in global immunization? Nat Med. 2003;9(1):99–103.
10. Rougier A, Rallis M, Krien P, Lotte C. In vivo percutaneous absorption: a key role for stratum corneum/vehicle partitioning. Arch Dermatol Res. 1990;282(8):498–505.
11. Bos JD, Meinardi MM. The 500 Dalton rule for the skin penetration of chemical compounds and drugs. Exp Dermatol. 2000;9(3):165–9.
12. Barry BW. Breaching the skin's barrier to drugs. Nat Biotechnol. 2004;22(2):165–7.
13. Prausnitz MR. Microneedles for transdermal drug delivery. Adv Drug Deliv Rev. 2004;56(5):581–7.
14. Henry S, McAllister DV, Allen MG, Prausnitz MR. Microfabricated microneedles: a novel approach to transdermal drug delivery. J Pharm Sci. 1998;87(8):922–5.
15. Martanto W, Davis SP, Holiday NR, Wang J, Gill HS, Prausnitz MR. Transdermal delivery of insulin using microneedles in vivo. Pharm Res. 2004;21(6):947–52.
16. Matriano JA, Cormier M, Johnson J, Young WA, Buttery M, Nyam K, et al. Macroflux microprojection array patch technology: a new and efficient approach for intracutaneous immunization. Pharm Res. 2002;19(1):63–70.
17. Park JH, Allen MG, Prausnitz MR. Biodegradable polymer microneedles: fabrication, mechanics and transdermal drug delivery. J Control Release. 2005;104(1):51–66.
18. Lee JW, Park JH, Prausnitz MR. Dissolving microneedles for transdermal drug delivery. Biomaterials. 2008;29(13):2113–24.
19. Sullivan SP, Koutsonanos DG, Del Pilar MM, Lee JW, Zarnitsyn V, Choi SO, et al. Dissolving polymer microneedle patches for influenza vaccination. Nat Med. 2010;16(8):915–20.
20. Matsuo K, Yokota Y, Zhai Y, Quan YS, Kamiyama F, Mukai Y, et al. A low-invasive and effective transcutaneous immunization system using a novel dissolving microneedle array for soluble and particulate antigens. J Control Release. 2012;161(1):10–7.
21. Matsuo K, Hirobe S, Yokota Y, Ayabe Y, Seto M, Quan YS, et al. Transcutaneous immunization using a dissolving microneedle array protects against tetanus, diphtheria, malaria, and influenza. J Control Release. 2012;160(3):495–501.

22. Draize J, Woodard G, Calvery H. Methods for the study of irritation and toxicity of substances applied topically to the skin and mucous membranes. J Pharmacol Exp Ther. 1944;82:377–90.
23. Barile FA. Validating and troubleshooting ocular in vitro toxicology tests. J Pharmacol Toxicol Methods. 2010;61(2):136–45.
24. Kunisawa J, Takahashi I, Okudaira A, Hiroi T, Katayama K, Ariyama T, et al. Lack of antigen-specific immune responses in anti-IL-7 receptor alpha chain antibody-treated Peyer's patch-null mice following intestinal immunization with microencapsulated antigen. Eur J Immunol. 2002;32(8):2347–55.
25. Hattori H, Yamaguchi F, Wagai N, Kato M, Nomura M. An assessment of antigenic potential of beta-lactam antibiotics, low molecular weight drugs, using guinea pig models. Toxicology. 1997;123(1–2):149–60.
26. Aida T, Ishikawa N, Shinkai K. Differences in immune responses to antibiotics in three guinea-pig strains. J Toxicol Sci. 1997;22(5):439–45.
27. Fregert S. Manual of contact dermatitis. 2nd ed. Copenhagen: Munksgaard; 1981.
28. Ivens U, Serup J, O'Goshi K. Allergy patch test reading from photographic images: disagreement on ICDRG grading but agreement on simplified tripartite reading. Skin Res Technol. 2007;13(1):110–3.
29. Kenney RT, Frech SA, Muenz LR, Villar CP, Glenn GM. Dose sparing with intradermal injection of influenza vaccine. N Engl J Med. 2004;351(22):2295–301.
30. Ansaldi F, Durando P, Icardi G. Intradermal influenza vaccine and new devices: a promising chance for vaccine improvement. Expert Opin Biol Ther. 2011;11(3):415–27.
31. Tada Y, Asahina A, Fujita H, Sugaya M, Tamaki K. Langerhans cells do not produce interferon-gamma. J Invest Dermatol. 2003;120(5):891–2.
32. Valladeau J, Saeland S. Cutaneous dendritic cells. Semin Immunol. 2005;17(4):273–83.
33. Van Damme P, Oosterhuis-Kafeja F, Van der Wielen M, Almagor Y, Sharon O, Levin Y. Safety and efficacy of a novel microneedle device for dose sparing intradermal influenza vaccination in healthy adults. Vaccine. 2009;27(3):454–9.

Fig. S1

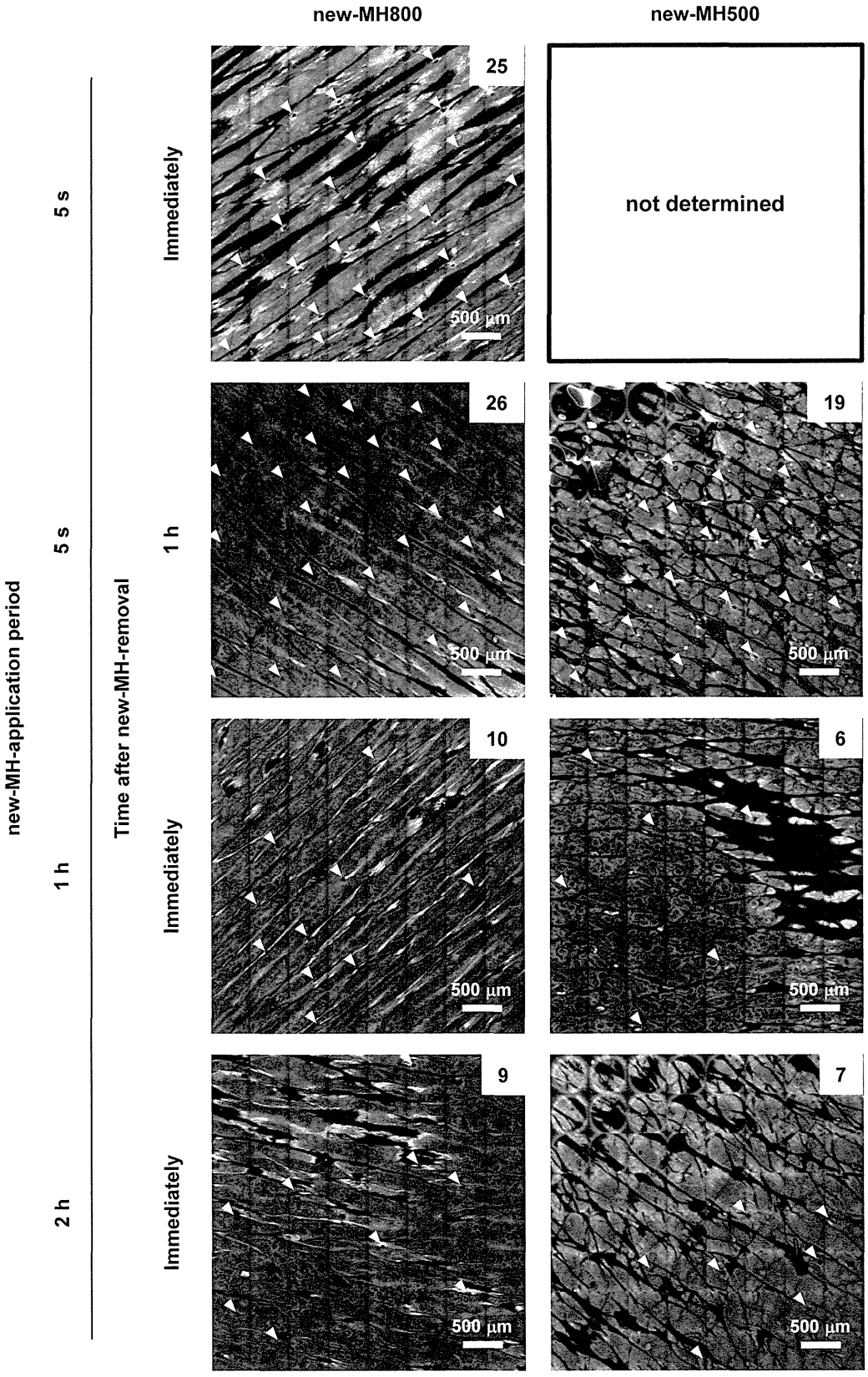
new-MH800
new-MH500
new-MH-application period
5 s
1 h
2 h
Time after new-MH-removal
Immediately
1 h
Immediately
Immediately
25
not determined
26
19
10
6
9
7
500 µm

Fig. S2

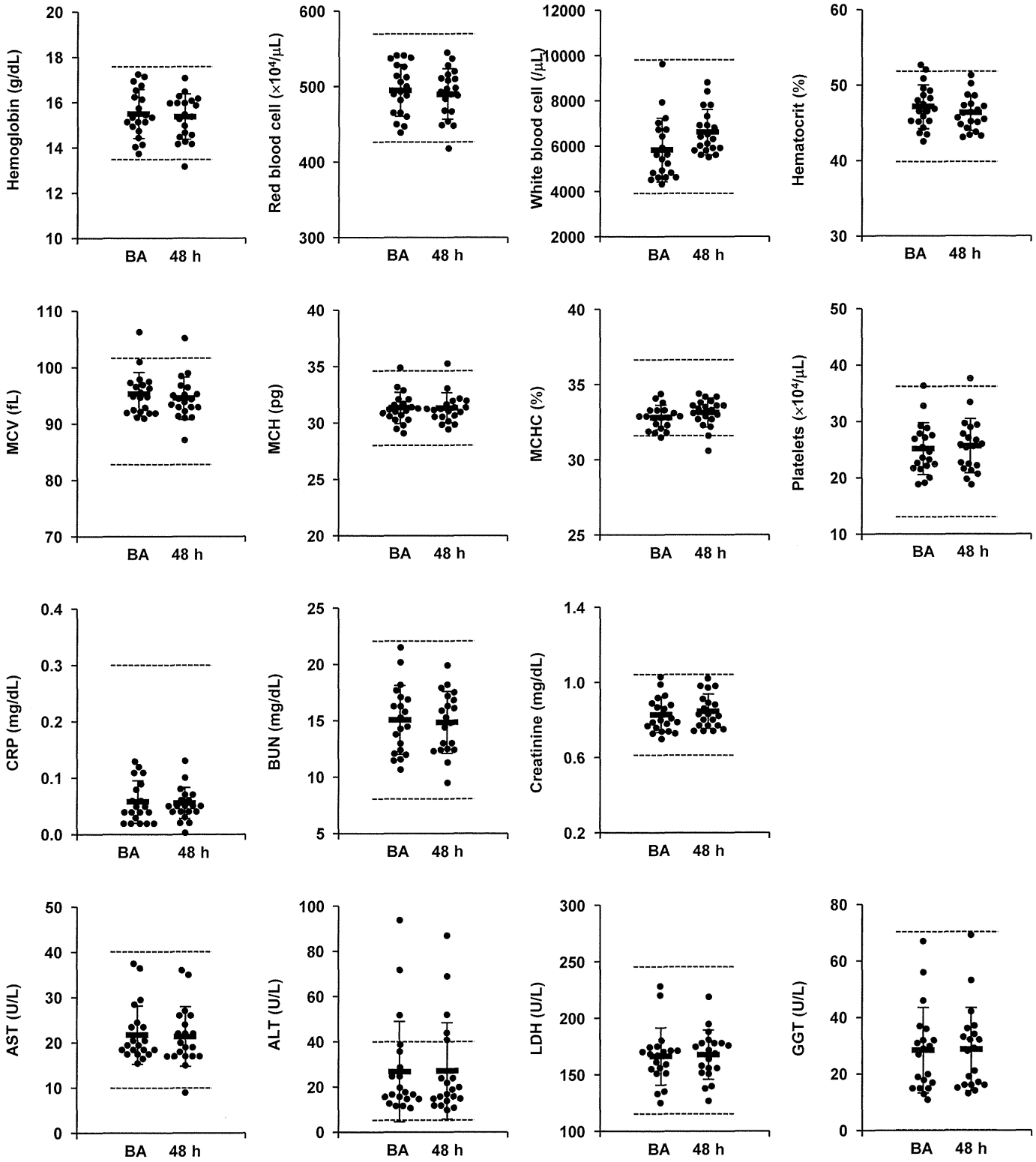
Hemoglobin (g/dL)
20
18
16
14
12
10
BA
48 h
Red blood cell (×10⁴/μL)
600
500
400
300
BA
48 h
White blood cell (/μL)
12000
10000
8000
6000
4000
2000
BA
48 h
Hematocrit (%)
60
50
40
30
BA
48 h
MCV (fL)
110
100
90
80
70
BA
48 h
MCH (pg)
40
35
30
25
20
BA
48 h
MCHC (%)
40
35
30
25
BA
48 h
Platelets (×10⁴/μL)
50
40
30
20
10
BA
48 h
CRP (mg/dL)
0.4
0.3
0.2
0.1
0.0
BA
48 h
BUN (mg/dL)
25
20
15
10
5
BA
48 h
Creatinine (mg/dL)
1.4
1.0
0.6
0.2
BA
48 h
AST (U/L)
50
40
30
20
10
0
BA
48 h
ALT (U/L)
100
80
60
40
20
0
BA
48 h
LDH (U/L)
300
250
200
150
100
BA
48 h
GGT (U/L)
80
60
40
20
0
BA
48 h

Journal of Controlled Release 171 (2013) 93–103

Contents lists available at SciVerse ScienceDirect

Journal of Controlled Release

journal homepage: www.elsevier.com/locate/jconrel

Development of a novel therapeutic approach using a retinoic acid-loaded microneedle patch for seborrheic keratosis treatment and safety study in humans

Yasuhiro Hiraishi [a], Sachiko Hirobe [a], Hiroshi Iioka [b], Ying-Shu Quan [c], Fumio Kamiyama [c], Hideo Asada [b], Naoki Okada [a,*], Shinsaku Nakagawa [a,**]

[a] Laboratory of Biotechnology and Therapeutics, Graduate School of Pharmaceutical Sciences, Osaka University, 1-6 Yamadaoka, Suita, Osaka 565-0871, Japan
[b] Department of Dermatology, Nara Medical University, 840 Shijo-cho, Kashihara, Nara 634-8522, Japan
[c] CosMED Pharmaceutical Co. Ltd., 32 Higashikujokawanishi-cho, Minami-ku, Kyoto 601-8014, Japan

ARTICLE INFO

Article history:
Received 14 November 2012
Accepted 9 June 2013
Available online 18 June 2013

Keywords:
Seborrheic keratosis
All-trans retinoic acid
Heparin-binding epidermal growth factor-like growth factor
Microneedle
Stratum corneum turnover

ABSTRACT

Seborrheic keratosis is one of the most common skin benign tumors in humans with a high occurrence rate of 80%–100% in people >50 years of age; however, its pathogenesis is still unclear. The standard treatment includes cryotherapy and laser surgery for physically removing lesions. Drug therapy for this condition has not been well established. We aimed to evaluate the use of all-trans retinoic acid (ATRA)-loaded microneedle (MN) patches as a simple, alternative therapeutic option to traditional surgical treatments. This therapeutic strategy was designed to induce the proliferation of basal keratinocytes and accelerate stratum corneum turnover, leading to the lesion falling off the surface of the skin. The MN patch induced epidermal hyperplasia and marked expression of heparin-binding epidermal growth factor-like growth factor mRNA and protein corresponding to ATRA activity in the skin of HR-1 hairless mice. The acceleration of stratum corneum turnover was also observed by the dansyl chloride method. The skin irritation study in mice and safety study in humans support the safety findings of our study. Overall, MN patches can offer an effective and safe means of ATRA delivery into the skin, and the ATRA-loaded MN patch appears to be an effective pharmaceutical product providing a novel therapeutic option for seborrheic keratosis.

1. Introduction

Seborrheic keratosis (SK) is one of the most common skin tumors in humans, with an occurrence rate of 80%–100% in people >50 years of age [1,2]. SK is characterized as sharply demarcated brownish plaques with verrucous surfaces. Originating from keratinocytes, they can develop anywhere on the skin excluding the palms and soles [3]. As this tumor is benign and not life-threatening, treatment is not mandatory. SK lesions may become irritated and itchy, and they are considered unattractive and disfiguring, which may have a significantly negative psychological impact. Therefore, the lesions are often removed for cosmetic reasons. Despite its occurrence frequency, a limited number of research papers on SK has been published [4,5], and the pathogenesis of SK is still unknown. Aging and cumulative exposure to sunlight were proposed as independent risk factors for the occurrence of SK [1,2]. Recently, somatic fibroblast growth factor receptor 3 (FGFR3) mutations have been identified in benign acanthotic skin tumors such as SKs and epidermal nevi. The spectrum of FGFR3 mutations in patients with multiple SKs has also been investigated [3].

Treatments for SK include cryotherapy and laser surgery. Cryosurgery using liquid nitrogen is the standard treatment for SK, and it is the most widely practiced method. The efficacy of cryosurgery depends on the thickness of the lesion, freeze time, and number of freeze–thaw cycles. Complications include scarring, hypopigmentation, and recurrence. Another surgical option is laser ablation such as that with erbium YAG or CO_2 lasers [4,6].

Drug therapy is also an attractive treatment option, but it is not well established. Retinoids are natural and synthetic metabolites and analogs of vitamin A. They are important regulators of epidermal proliferation and differentiation [7,8]. Twice-daily topical application of 0.1% tazarotene cream, that is retinoid, resulted in clinical and histological improvement of SK in seven of 15 patients. In these seven

Abbreviations: SK, seborrheic keratosis; FGFR3, somatic fibroblast growth factor receptor 3; ATRA, all-trans retinoic acid; HB-EGF, heparin-binding epidermal growth factor-like growth factor; EGFR, epidermal growth factor receptor; MN, microneedle; HE, hematoxylin and eosin; EVG, Elastica van Gieson; CRABPII, cellular retinoic acid binding protein II; IL-1β, interleukin-1β; TNF-α, tumor necrosis factor-α; IL-6, interleukin-6; GAPDH, glyceraldehyde-3-phosphate dehydrogenase; CT, threshold cycle number; UV, ultraviolet; SCT, stratum corneum turnover; ICDRG, International Contact Dermatitis Research Group; HSD, honestly significant difference.

* Corresponding author. Tel./fax: +81 6 6879 8176.
** Corresponding author. Tel.: +81 6 6879 8175; fax: +81 6 6879 8179.
E-mail addresses: okada@phs.osaka-u.ac.jp (N. Okada), nakagawa@phs.osaka-u.ac.jp (S. Nakagawa).

0168-3659/$ – see front matter © 2013 Elsevier B.V. All rights reserved.
http://dx.doi.org/10.1016/j.jconrel.2013.06.008

patients, the application site was indistinguishable from normal skin, and these sites displayed no SK lesions histologically [9]. In another study, topical 0.075% retinoic acid solution, 5% 5-fluorouracil cream, and calcipotriol cream were applied to SK-like lesions for 6 weeks. Retinoic acid appeared to be associated with the best clinical results. However, complete remission was not achieved [10].

All-trans retinoic acid (ATRA), a natural retinoid, is the major biologically active form of retinoids. ATRA has several significant biological effects on the epidermis and dermis [11,12]. Heparin-binding epidermal growth factor-like growth factor (HB-EGF) is a human growth factor capable of binding to the epidermal growth factor receptor (EGFR). EGFR can be localized throughout the entire epidermis and plays an important role in re-epithelialization by increasing keratinocyte proliferation and cell migration in wounded skin [13]. ATRA induces HB-EGF expression in mice suprabasal keratinocytes [14,15], human keratinocytes, and organ-cultured skin, suggesting that epidermal hyperplasia following ATRA treatment may be mediated by keratinocyte-derived HB-EGF [7,16]. Thus, ATRA increases the proliferation of basal keratinocytes, inducing the accelerated turnover of epidermal cells and epidermal thickening indirectly [17]. These effects could be beneficial in the treatment of SK.

Although ATRA has drawn interest in the treatment of dermatological diseases such as acne and psoriasis, some drawbacks such as its poor water solubility and photostability and skin irritation reactions limit its topical use [18–20]. Furthermore, the skin permeability of ATRA is relatively low; the permeability of Retin-A, a commercially available ATRA cream, was 5% in newborn pig skin [21]. To overcome these disadvantages, we recently developed ATRA-loaded microneedle (MN) patches consisting of micron-scale needles assembled on a transdermal patch [22]. Over the past 15 years, the field of MN technology has rapidly progressed, with more than 350 research papers being published [23]. This technology provides a reliable and promising transcutaneous delivery system for both low-molecular-weight molecules and macromolecules. The majority of research papers published thus far used non-dissolving MNs. Metal-based MNs coated with water-soluble formulations facilitate the successful delivery of agents such as hepatitis B surface antigen [24], inactivated influenza virus [25], influenza virus-like particle [26], bacillus Calmette–Guérin [27], and live-attenuated measles virus [28] into the skin. Polymer MNs that dissolve in the skin have also been developed; these MNs display successful delivery and efficacy [29–32]. In our earlier study, ATRA-loaded dissolving polymer MN patches exhibited good stability and facilitated ATRA delivery into mouse skin with a delivery rate of >90%, indicating that the ATRA-loaded MN patch developed by us would be an effective pharmaceutical product providing a novel transcutaneous ATRA delivery system for the skin [22]. Thus, we hypothesized that ATRA delivery into the keratinocyte layer using MN patches may accelerate epidermal cell turnover and stratum corneum turnover (SCT), resulting in SK lesions falling off the surface of the skin, potentially representing a novel therapeutic approach for SK treatment. This strategy would also benefit patients that are treated unsuccessfully by the standard treatment of cryosurgery. In addition, most of the patients for SK are older people, and they may need to go to the hospital several times to undergo surgical treatment. Potential self administration by MN would ease the burden for aged patients.

In the present study, we attempted to develop a dissolving polymer MN patch as a simple and reliable delivery technology for ATRA that could provide a novel and alternative therapeutic option to traditional surgical treatment for SK.

2. Materials and methods

2.1. Animals

Nine-week-old female HR-1 hairless mice were purchased from SHIMIZU Laboratory Supplies Co., Ltd. (Kyoto, Japan). Animals were housed at the Osaka University animal facility. All animal studies were conducted in accordance with the guidelines provided by the Animal Care and Use Committee of Osaka University.

2.2. Fabrication of the dissolving ATRA-loaded MN patch

As described previously [22,33], the dissolving MN patch was fabricated at CosMED Pharmaceutical Co. Ltd. (Kyoto, Japan) using micromolding technologies with sodium hyaluronate as the base material. In brief, sodium hyaluronate (JP grade, Kikoman Biochemifa Company, Tokyo, Japan), dextran 70 (JP grade, Meito Sangyo, Nagoya, Aichi), and Polyvidone (JPE grade, BASF Japan, Tokyo, Japan) were dissolved in distilled water at a ratio of 11:8:1 and mixed with ATRA (Sigma-Aldrich Inc., St. Louis, MO, USA). The aqueous solution was casted on micromolds and dried in a desiccator at room temperature. The dissolving ATRA-loaded MN patches were obtained by removing them from the micromolds. Placebo dissolving MN patches lacking ATRA were also fabricated in the same manner. To form the MN transcutaneous patch system, patches with an area of 0.8 cm^2 were fixed onto an adhesive film with a surface area of 2.3 cm^2. Our dissolving MN patch system consisted of the MicroHyala® patch with MNs that were 300 (MH300) or 800 μm (MH800) in length. The amount of ATRA loaded onto the MN patch was determined using a high-performance liquid chromatography method as reported previously [22,34].

2.3. Administration of ATRA in mice

The back skin of one group of HR-1 hairless mice was pierced with the ATRA-loaded MN patch (MH300, 1.4 μg of ATRA) using a hand-held applicator [33]. The patch was left in place for 120 min and covered with wound management film (BIOCLUSIVE; Johnson & Johnson Medical, Ltd., Tokyo, Japan). The amount of ATRA delivered into the skin was approximately 1.6 μg per cm^2 in consideration of the following: 1.4 μg of ATRA loaded into each MN patch, patch area of 0.8 cm^2, and efficiency of ATRA delivery into the mouse skin of 92% [22]. The second group of mice received placebo MN patches (without ATRA) in the same manner as the ATRA-loaded MN patch group. The third group of mice received ATRA acetone solution (1.6 μg of ATRA/25 μl) onto a 1-cm^2 area of their back skin as a positive control group. Selection of the positive control was referring to the previous publication by Xiao et al. [14], and acetone as a vehicle for ATRA has been recommended for these types of studies to provide sufficient skin penetration of ATRA [35]. Sham-administrated mice received 25 μl of acetone onto their back skin (1 cm^2). Intact (untreated) mice served as negative controls in this study. Administration was repeated once daily for 4 days at the same site. Twelve hours after the final administration, the skin of the administration site was photographed for a skin irritation study, and then harvested and subsequently used for histological evaluation, real-time reverse transcription polymerase chain reaction (RT-PCR) analysis, and fluorescent immunohistochemical staining assessments. All treatments were performed under isoflurane inhalation anesthesia.

2.4. Histological examination of skin

The skin harvested from the mice was fixed in 10% neutral-buffered formalin at pH 7.4 (Wako Pure Chemical Industries, Ltd., Osaka, Japan) and embedded in paraffin. Five-micrometer-thick skin sections were subjected to hematoxylin and eosin (HE) or elastica van Gieson (EVG) staining. The preparation of skin sections, staining, and histological evaluation were conducted at the Applied Medical Research Laboratory (Osaka, Japan). Bright-field images of stained skin sections were captured by a bright-field microscope (BZ-8000; Keyence Corporation, Osaka, Japan).

2.5. Real-time RT-PCR

Gene expression was quantified by real-time RT-PCR using TaqMan® Gene Expression Assays (Applied Biosystems, Foster City, CA, USA) on the CFX96 real-time PCR detection system (Bio-Rad, Hercules, CA, USA). Skin sections harvested from the mice were cut into small pieces and then homogenized in Sepasol RNA I Super G (Nacalai Tesque, Kyoto, Japan), and total RNA was isolated according to the manufacturer's instructions. The RT procedure was conducted as follows: annealing for 10 min at 30 °C, extension at 20 min at 42 °C, and denaturation at 5 min at 99 °C in 20 μl of reaction mixture containing 0.5 μg of total RNA treated with DNase I, 4 μl of 5× RT buffer (including 25 mM $MgCl_2$), 2 μl of a dNTP mix (1 mM each), 1 μM random primer (9-mer), 1 μM oligo$(dT)_{20}$, and 100 U of ReverTra Ace (TOYOBO Co., Ltd., Osaka, Japan). Amplifications were performed in a total volume of 20 μl composed of TaqMan universal PCR master mix II (Applied Biosystems), TaqMan probe (Applied Biosystems), and 50 ng of cDNA under the thermal cycling conditions of 50 °C for 2 min and 95 °C for 10 min followed by 45 cycles of 95 °C for 15 s and 60 °C for 1 min. The following TaqMan probes were used in this study: HB-EGF (Mm00439307_m1), cellular retinoic acid binding protein II (CRABPII; Mm00801691_m1), interleukin-1β (IL-1β; Mm01336189_m1), tumor necrosis factor-α (TNF-α; Mm00443258_m1), interleukin-6 (IL-6; Mm99999064_m1), and glyceraldehyde-3-phosphate dehydrogenase (GAPDH; Mm99999915_g1). The threshold cycle number (CT) value was used to calculate the relative amount of mRNA according to the $2^{-\Delta\Delta CT}$ method [36]. The CT value of each target gene was normalized to the endogenous RNA levels of the housekeeping reference gene GAPDH. The values represent the fold change of the gene in the treatment group relative to that in the untreated group. Similar data were obtained when the values were standardized to β-actin (Mm00607939_s1; data not shown).

2.6. Fluorescent immunohistochemical staining of HB-EGF protein

The skin harvested from mice was frozen in OCT compound (Sakura Finetechnical Co., Ltd., Tokyo, Japan) and cut into 5-μm-thick sections using a cryostat. Sections were then fixed in acetone for 10 min and air-dried. Nonspecific immunoreactivity was blocked by incubation in Tris-buffered saline containing 0.1% Tween-20 (TBST) with 3% bovine serum albumin (Sigma-Aldrich) for 1 h. The primary antibody used was rabbit-anti HB-EGF (sc-28908, Santa Cruz Biotechnology, Inc., Santa Cruz, CA, USA) diluted 1:50 with antibody diluent with background-reducing components (s3022, Dako, Tokyo, Japan). The sections were incubated with the primary antibody for 1 h and then washed in TBST. The secondary antibody used was Alexa Fluor 488 goat-anti-rabbit IgG (A-11034, Invitrogen, Carlsbad, CA, USA) diluted 1:200 with antibody diluent with background-reducing components. After 1 h of incubation with the secondary antibody, the sections were washed in TBST and mounted with Prolong Gold antifade reagent with DAPI (Invitrogen). Histological examination was performed using a fluorescence microscope (BZ-8000).

2.7. In vivo skin irritation study in mice

To evaluate skin irritation induced by the application of ATRA using MN patches, the administration sites were observed and scored for signs of erythema or edema according to the Draize dermal scoring criteria [33,37] 12 h after the final application. The Draize scoring system scores the presence of erythema and edema as follows: 0, no erythema or edema; 1, very slight erythema and/or barely perceptible edema; 2, well-defined erythema and/or slight edema; 3, moderate to severe erythema or moderate edema, and 4, severe erythema and/or edema.

2.8. SCT time

The SCT time was estimated by the dansyl chloride staining method [38,39]. Dansyl chloride (5-dimethylaminonaphthalene-1-sulfonyl chloride, Sigma Chemical Co.) was finely dispersed at 5% (wt/wt) in Vaseline (JP grade) and then applied to the back skin of HR-1 hairless mice occlusively using a Finn Chamber (SmartPractice, Phoenix, AZ, USA) for 24 h. After removal of the Finn Chamber, dansyl chloride deposited on the skin surface was removed using ethanol. For one group of mice, an ATRA-loaded MN patch (MH300, 1.4 μg of ATRA) was pressed into the skin of each mouse at the staining site and left in place for 120 min covered with wound management film, after which the MN patch was removed from the skin. The second group of mice received placebo MN patches (without ATRA) in the same manner. The third group of mice received ATRA acetone solution (1.6 μg of ATRA/25 μl) on the stained skin as a positive control. After a single application of ATRA-loaded or placebo MNs, the skin of mice was visually examined under an ultraviolet (UV) lamp (VL-6L, Vilber Lourmat, France). UV-induced fluorescence images corresponding to dansyl chloride staining were obtained using the Cri Maestro EX *in vivo* imaging system (Cambridge Research and Instrumentation, Woburn, MA, USA). To capture the image, a blue emission filter was used at 515 nm. The exposure time was 400 ms, and the spectral resolution for all imaging was 10 nm. The SCT time was expressed as the time in days from administration until the disappearance of fluorescence. All treatments in animals were performed under isoflurane inhalation anesthesia.

2.9. Safety study in humans

To evaluate the safety of ATRA-loaded MN patches (MH800, 1.6 μg of ATRA), four healthy volunteers (36–60 years old; Asian; two males and two females) were enrolled after providing informed consent. All procedures in humans were performed at Nara Medical University in accordance with a protocol approved by the ethics committee of Nara Medical University. An ATRA-loaded MN patch was pressed into the skin of each volunteer using a handheld applicator and left in place for 6 h. After removal of the patch, to assess adverse reactions related to ATRA-loaded MN patch application, the skin irritation reaction was scored according to the classification of the International Contact Dermatitis Research Group (ICDRG) system [40]. A general blood test and biochemical tests of liver and renal function were performed to evaluate the presence of systemic adverse reactions.

2.10. Statistical analysis

The obtained data were analyzed using Tukey–Kramer's honestly significant difference (HSD) test and analysis of variance (ANOVA) by JMP software ver. 8.0 (SAS Institute Inc., Cary, NC, USA). In all cases, $p < 0.05$ was considered significant.

3. Results

3.1. HE and EVG staining for histological evaluation

Our previous study demonstrated that MNs successfully penetrate the skin barrier and deliver ATRA into the mouse skin [22]. Topical application of ATRA induces a marked increase in epidermal thickness and causes epidermal hyperplasia [12]. The ability of the ATRA-loaded MN patches to induce epidermal hyperplasia was evaluated in mice after four repeated treatments. Epidermal hyperplasia was observed in the HE-stained sections of the administration sites of mice in the ATRA-loaded MN patch, placebo MN patch, and ATRA acetone solution groups (Fig. 1A–E). Epidermal hyperplasia was also measured quantitatively by epidermal thickness in three different locations for six animals for each treatment group using bright-field

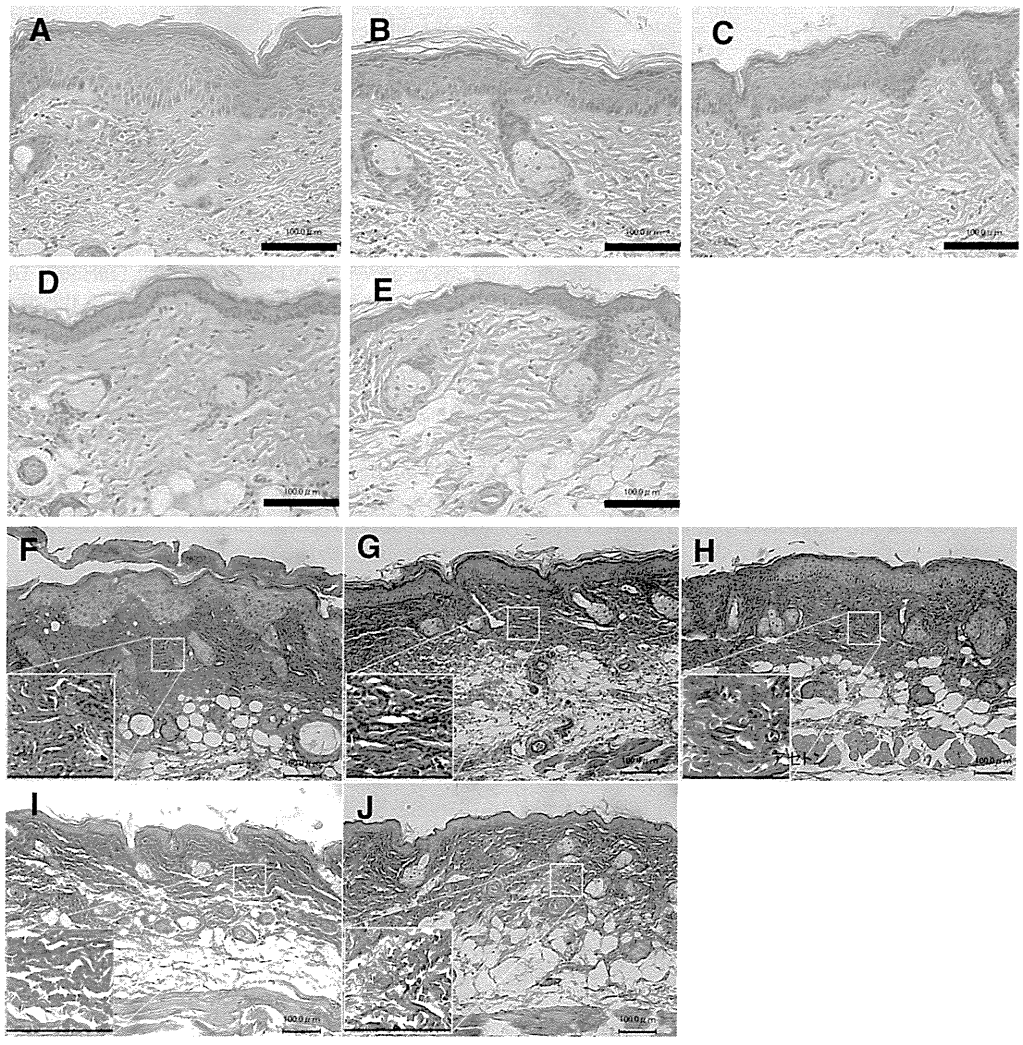
A
B
C
D
E
F
G
H
I
J

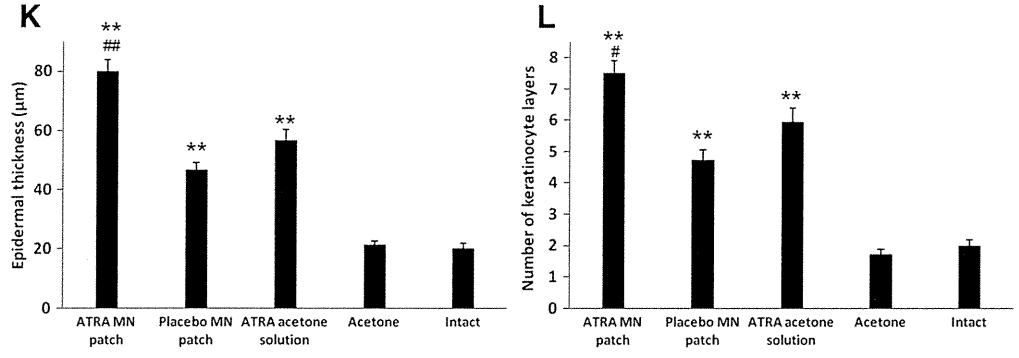
K
Epidermal thickness (μm)
0
20
40
60
80
** ##
**
**
ATRA MN patch
Placebo MN patch
ATRA acetone solution
Acetone
Intact
L
Number of keratinocyte layers
0
1
2
3
4
5
6
7
8
** #
**
**
ATRA MN patch
Placebo MN patch
ATRA acetone solution
Acetone
Intact

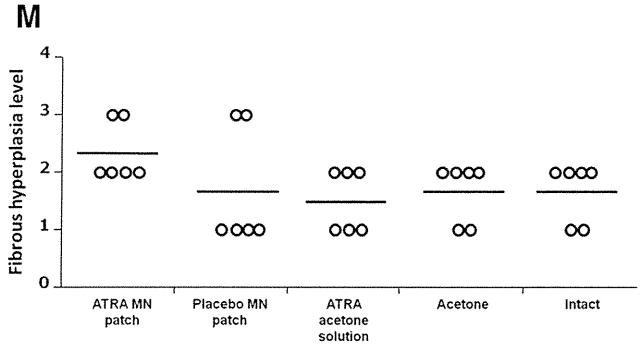
M
Fibrous hyperplasia level
0
1
2
3
4
ATRA MN patch
Placebo MN patch
ATRA acetone solution
Acetone
Intact

stereomicroscopy (VHX-1000; Keyence Corporation). Epidermal thickness was significantly increased in the skin of mice treated with ATRA-loaded MN patches, placebo MN patches, or ATRA acetone solution compared with the findings of sham-treated and untreated mice (Tukey–Kramer's HSD test, $p < 0.01$) (Fig. 1K). The group treated with ATRA-loaded MN patches displayed the most significant increase in epidermal thickness among all groups evaluated, and the difference in epidermal thickness between the ATRA-loaded MN patch and ATRA acetone solution groups was significant (Tukey–Kramer's HSD test, $p < 0.01$). In addition, no significant difference in epidermal thickness was observed between the placebo MN and ATRA acetone solution groups (Tukey–Kramer's HSD test, $p > 0.05$). Furthermore, the results regarding the number of keratinocyte layers corresponded to those of epidermal thickness (Fig. 1L). These results suggest that ATRA-loaded MN patches can effectively induce epidermal hyperplasia. Sham treatment with acetone did not increase the number of keratinocyte layers or epidermal thickness in comparison with the findings in the untreated group (Tukey–Kramer's HSD test, $p > 0.05$), which also indicates that acetone is a negligible factor in the induction of keratinocyte proliferation by ATRA acetone solution, as previously reported [14].

Next, we evaluated whether the ATRA-loaded MN patches stimulate collagen synthesis in the dermis using EVG-stained sections. Collagenous fibers and elastic fibers were stained red and black by EVG, respectively (Fig. 1F–J). Increased dense staining corresponding to collagen in the dermis was observed in the ATRA-loaded MN patch group (Fig. 1F). The level of hyperplasia in collagenous and elastic fibers was scored by the third party research organization Applied Medical Research Laboratory (Fig. 1M). These results indicate that the ATRA-loaded MN patch can potentially stimulate collagen synthesis in the dermis, but significant difference of the score compared to the intact group was not obtained in this study.

3.2. HB-EGF and CRABPII induction after the application of ATRA-loaded MN patches

To investigate whether ATRA-loaded MN patch application can induce HB-EGF expression in the epidermis and dermis of mice, we compared HB-EGF mRNA expression levels between ATRA-loaded MN-treated skin and untreated skin. Fig. 2A shows that both ATRA-loaded MN patch and ATRA acetone solution treatment significantly induced HB-EGF mRNA expression compared to its expression in untreated skin (5.1- and 6.7-fold, respectively; Tukey–Kramer's HSD test, $p < 0.01$), whereas HB-EGF mRNA expression in the ATRA-loaded MN patch and ATRA acetone solution groups was comparable (Tukey–Kramer's HSD test, $p > 0.05$). Placebo MN patch application also led to a 1.9-fold induction of HB-EGF mRNA compared with its expression in untreated skin, but the difference was not significant.

Then, we evaluated HB-EGF protein expression using a fluorescent immunohistochemical staining method. Fluorescence micrographs of histological sections after staining demonstrated that HB-EGF expression (green) in the epidermis, particularly in keratinocyte layers, was induced by the application of ATRA-loaded MN patches, placebo MN patches, or ATRA acetone solution; however, an intense green spot corresponding to HB-EGF was not observed in untreated skin (Fig. 2C–G). Furthermore, ATRA application using MN patches or acetone solution induced HB-EGF expression in the epidermis and dermis (Fig. 2C and E).

HB-EGF mRNA expression is also induced in the wound healing process in normal human epidermal keratinocytes and mice skin [41]. MNs can create many micron-scale holes on the skin, which may be considered wounds. Thus, marked HB-EGF mRNA expression induced by ATRA-loaded MN patches may include two factors, i.e., ATRA-derived and wound-derived HB-EGF mRNA. To better understand the ATRA activity of our developed ATRA-loaded MN patch, we evaluated CRABPII mRNA expression, which can be used as a reliable and selective marker for ATRA activity in the skin [42]. Fig. 2B illustrates that the ATRA-loaded MN patches significantly induced CRABPII mRNA expression compared with its expression in untreated skin (9.7-fold; Tukey–Kramer's HSD test, $p < 0.01$), and the relative expression level was comparable to that induced by ATRA acetone solution (9.5-fold). Furthermore, the difference in CRABPII mRNA expression levels between ATRA-loaded MN patch and placebo MN patch application was significant (Tukey–Kramer's HSD test, $p < 0.01$).

These results indicate that ATRA-loaded MN patches can induce pronounced HB-EGF mRNA and protein expression in mice skin, and the activity of ATRA delivered by ATRA-loaded MN patches was confirmed by CRABPII mRNA expression assay.

3.3. In vivo skin irritation in mice caused by ATRA-loaded MN patches

We evaluated erythema and edema at the administration sites on the back skin of mice 12 h after the final of four repeated applications. Fig. 3A reveals that very slight erythema associated with ATRA-loaded and placebo MN patch application was observed at the administration site, whereas ATRA acetone solution administration caused moderate to severe erythema. Edema was not observed in any treatment group. Next, we scored the degree of erythema using the Draize dermal scoring system. The degree of erythema caused by ATRA-loaded MN patches was comparable to that caused by placebo MN patches and lower than that caused by ATRA acetone solution (Fig. 3B). Acetone application in the sham group resulted in almost no erythema, similar to the findings in the intact group.

To further evaluate the cause of skin irritation, pro-inflammatory cytokine (IL-1β, TNF-α, IL-6) mRNA expression was evaluated in mice. Fig. 3C demonstrates that IL-1β mRNA expression was significantly increased by ATRA-loaded and placebo MN patch application compared with that in the intact group (Tukey–Kramer's HSD test, $p < 0.05$). ATRA acetone solution also induced IL-1β mRNA expression by 3.6-fold, but this induction was not significant compared with the expression in the intact group (Tukey–Kramer's HSD test, $p > 0.05$). TNF-α mRNA expression displays similar trend to that of IL-1β, which increased compared with that in the intact group on ATRA-loaded and placebo MN patch application, but not significant (Tukey–Kramer's HSD test, $p > 0.05$) (Fig. 3D). Fig. 3E reveals that all three treatments excepting acetone treatment group induced IL-6 mRNA expression significantly compared with that in the intact group (Tukey–Kramer's HSD test, $p < 0.05$). Among the three treatment groups, the highest IL-6 mRNA expression level was induced by ATRA acetone solution, but the differences in IL-6 mRNA expression among the treatment groups were not significant. These results suggest that the ATRA MN patch can potentially cause mild erythema and increase pro-inflammatory cytokine mRNA levels in mice. An

Fig. 1. HE and EVG staining for histological evaluation. HE staining of HR-1 hairless mouse skin after the application of (A) ATRA-loaded MN patches, (B) placebo MN patches, (C) ATRA acetone solution, (D) acetone, or (E) no treatment (intact). Skin sections (5 μm thick) were photographed using a bright-field microscope. Epidermal hyperplasia was identified in mice treated with ATRA-loaded MN patches, placebo MN patches, and ATRA acetone solution. Scale bar, 100 μm. EVG staining of HR-1 hairless mouse skin after the application of (F) ATRA-loaded MN patches, (G) placebo MN patches, or (H) ATRA acetone solution (I) acetone, or (J) no treatment. Skin sections (5 μm thick) were photographed using a bright-field microscope. Collagenous fibers were stained red. Elastic fibers were stained black. Scale bar, 100 μm. Epidermal hyperplasia at the application site, measured quantitatively by (K) epidermal thickness and (L) the number of keratinocyte layers. Data represent the average ± SD of 18 measurements in three different locations from one tissue section for 6 mice for each treatment group. $^{**}p < 0.01$ vs. intact, $^{\#\#}p < 0.01$ vs. ATRA acetone solution, $^{\#}p < 0.05$ vs. ATRA acetone solution. (M) Fibrous hyperplasia level assessed by histological examination on EVG-stained sections. Hyperplasia was scored as follows: 0: no fibrous hyperplasia 1: very slight or barely perceptible fibrous hyperplasia 2: slight fibrous hyperplasia 3: moderate fibrous hyperplasia 4: severe fibrous hyperplasia. Data represent one tissue section for 6 mice for each treatment group. The mean value is shown as a bar.

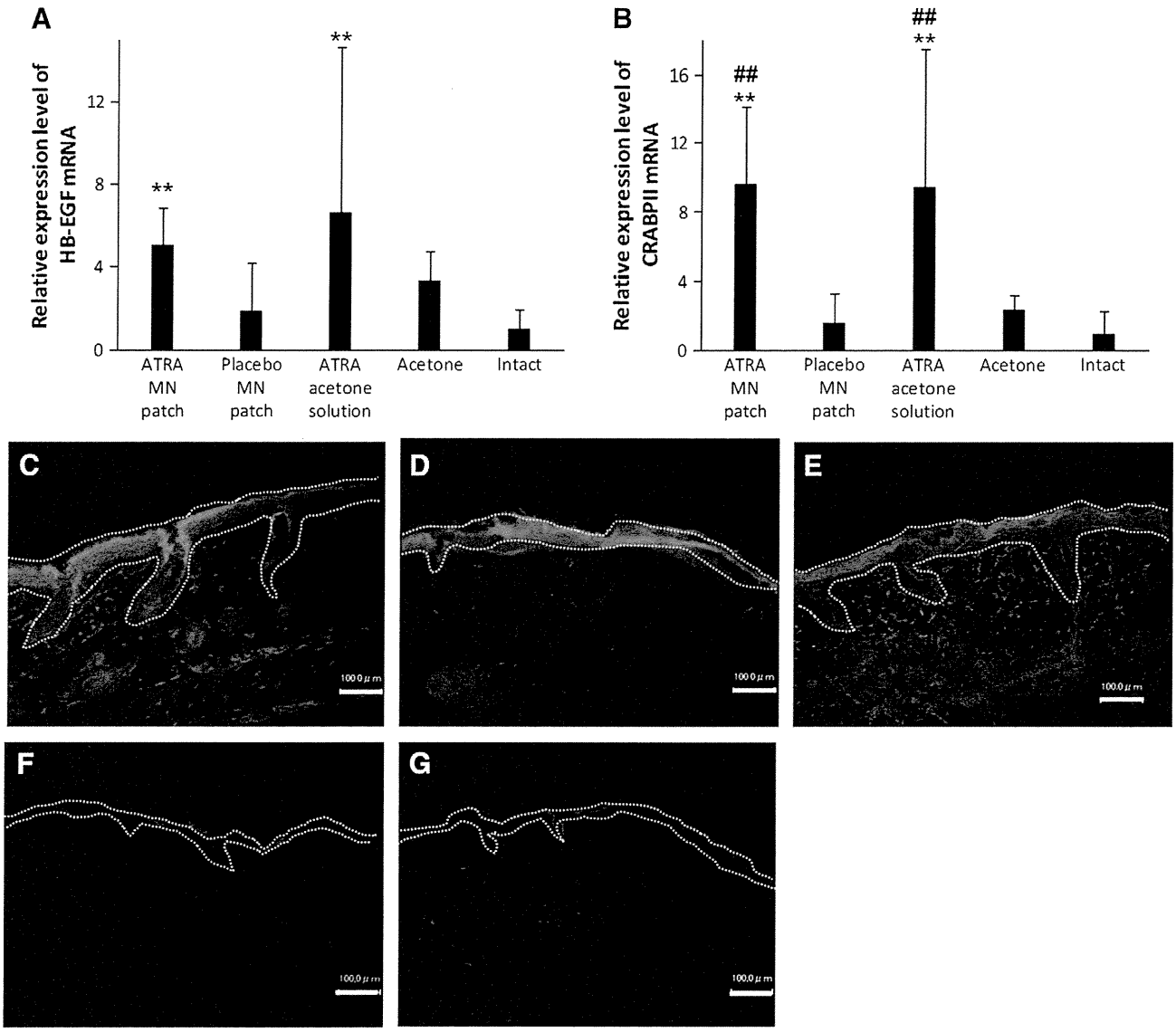

Fig. 2. HB-EGF and CRABPII induction after the application of ATRA-loaded MN patches. Effect of treatment on (A) HB-EGF and (B) CRABPII mRNA expression in HR-1 hairless mice 12 h after the final of four repeated applications of ATRA-loaded MN patches, placebo MN patches, ATRA acetone solution, or acetone as assayed by real-time PCR. Values indicate the relative mRNA level of each target gene normalized to its expression in the intact group. GAPDH expression was used as an endogenous control. Data represent the average ± SD of six measurements. Logarithmic transformations of the data were made to achieve normalcy before statistical analysis; however, the figures depict the data on the untransformed scale. $^{**}p < 0.01$ vs. intact, $^{\#\#}p < 0.01$ vs. placebo MN patch. HB-EGF expression was assessed by fluorescent immunohistochemical staining of the skin sections of HR-1 hairless mice after treatment with (C) ATRA-loaded MN patches, (D) placebo MN patches, (E) or ATRA acetone solution, (F) acetone, or (G) no treatment (intact). Twelve hours after the final of four repeated treatments, the skin was harvested and frozen. Sections (5 μm thick) were subjected to hybridization using a rabbit-anti HB-EGF primary antibody and an Alexa Fluor 488 goat-anti-rabbit IgG secondary antibody. Histological sections were photographed using a fluorescence microscope. HB-EGF was stained green. The white dotted lines denote the surfaces between the stratum corneum and epidermis and between the epidermis and superficial dermis from top to bottom. Scale bar, 100 μm.

obvious correlation between the degree of erythema and cytokine mRNA expression levels was not identified in this study.

3.4. SCT time acceleration by the ATRA-loaded MN patch

To evaluate whether ATRA-loaded MN patches shorten the SCT time in mice, SCT was assessed by the dansyl chloride method. After staining the stratum corneum of the back skin of mice with dansyl chloride, a single treatment was performed on the staining site using ATRA-loaded MN patches, placebo MN patches, or ATRA acetone solution. Fluorescent images demonstrated that the UV-induced green spot corresponding to dansyl chloride staining disappeared 6 days after ATRA-loaded MN patch application (Fig. 4A). Similar results were also obtained for ATRA acetone solution treatment, whereas a small green spot remained 6 days after placebo MN patch application as well as in the intact group. Fig. 4B shows the SCT time expressed as the time in days from administration until the disappearance of fluorescence corresponding to dansyl chloride staining. ATRA-loaded MN patch application significantly shortened the SCT time (6.5 days) compared with the findings in the placebo MN and intact groups (Tukey–Kramer's HSD test, $p < 0.05$). The SCT time in the ATRA-loaded MN groups was also comparable with that in ATRA acetone solution group. These results indicate that ATRA-loaded MN patch application accelerated SCT in mice.

3.5. Safety study in humans

Because appropriate animal models of SK lesions have not been established yet to the best of our knowledge, the efficacy of ATRA-loaded MN patches for SK therapy needs to be evaluated in humans. Prior to the human efficacy study, we investigated the safety of

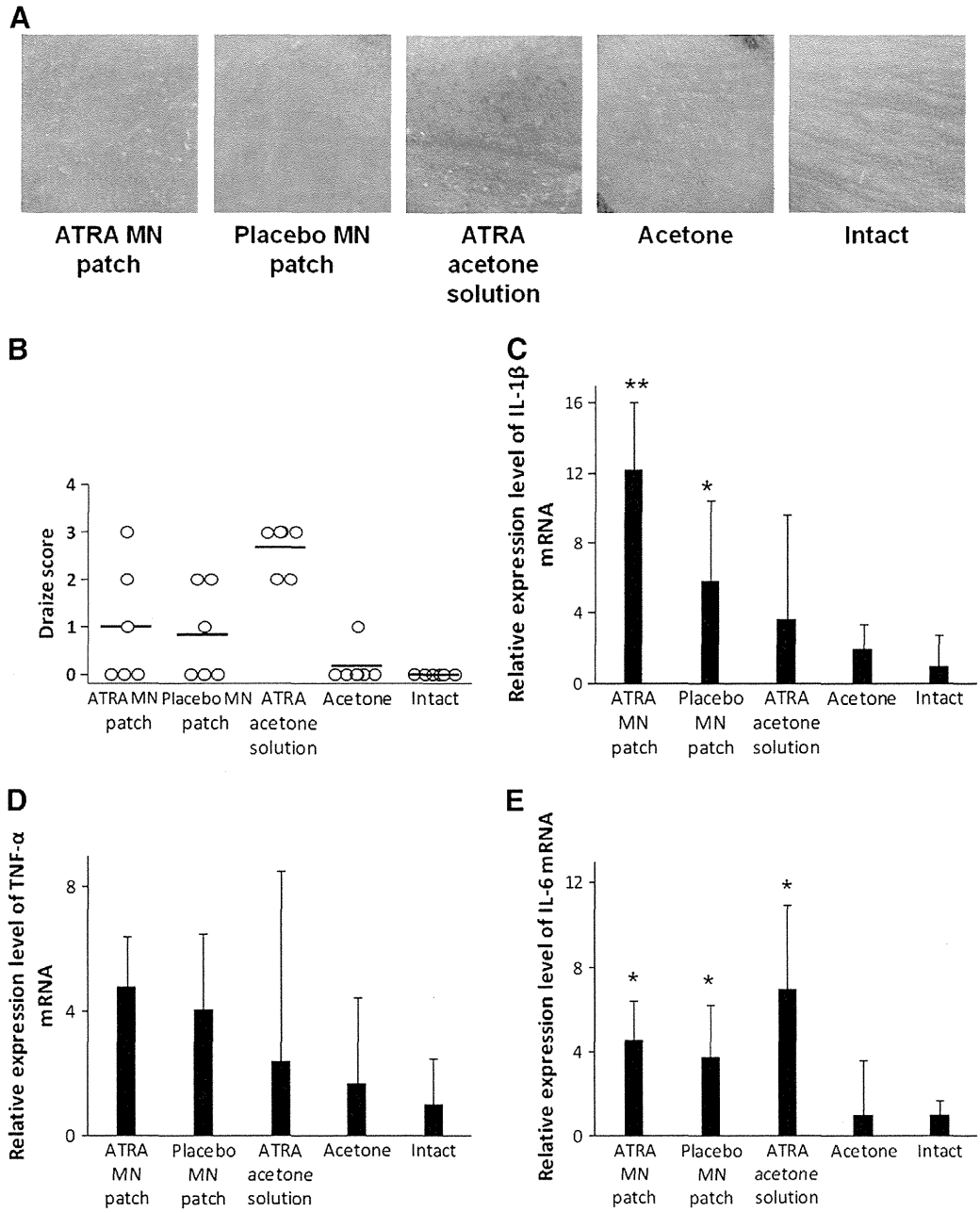

Fig. 3. *In vivo* skin irritation in mice caused by ATRA-loaded MN patches. Administration sites on the back skin of HR-1 hairless mice were observed and scored for signs of erythema or edema 12 h after the final of four repeated applications of ATRA-loaded MN patches, placebo MN patches, ATRA acetone solution, or acetone. (A) Representative photographs of the skin surface (1 cm × 1 cm). (B) The degree of erythema or edema was scored using the Draize dermal scoring system as follows: 0: no erythema or edema 1: very slight erythema and/or barely perceptible edema 2: well-defined erythema and/or slight edema 3: moderate to severe erythema or moderate edema 4: severe erythema and/or edema. The mean value is shown as a bar. mRNA expression of (C) IL-1β, (D) TNF-α, and (E) IL-6 in HR-1 hairless mice 12 h after the final of four repeated applications of ATRA-loaded MN patches, placebo MN patches, ATRA acetone solution, or acetone as assayed by real-time PCR. Values indicate the relative mRNA level of each target gene normalized to its expression in the intact group. GAPDH expression was used as an endogenous control. Data represent the average ± SD of six measurements. Logarithmic transformations of the data were made to achieve normalcy before statistical analysis; however, the figures depict the data on the untransformed scale. $^{**}p < 0.01$ vs. intact, $^{*}p < 0.05$ vs. intact.

ATRA-loaded MN patches in healthy human volunteers. Four subjects were enrolled in this study, and each volunteer received a single application of the patch. The patch was left in place for 6 h to allow MNs to dissolve well (Fig. 5). After removal of the patch, localized adverse events were categorized on the basis of the degree of skin irritation using the ICDRG system, and systemic adverse effects were evaluated using general blood tests and biochemical tests. Immediately after patch removal (time 0), a weak positive reaction indicating erythema due to patch application was identified in all four subjects (Fig. 6). However, seven days after the application, most reactions disappeared, and the skin completely recovered to normal at 30 days after the application (Table 1). In addition, patch application did not have systemic adverse effects, as determined by blood testing. None of the subjects particularly showed any adverse symptom. Thus, these data indicate that our developed ATRA-loaded MN patch potentially do not cause serious adverse events, although the number of enrolled subjects in this study were limited.

4. Discussion

Therapeutic interest in ATRA as a dermatological treatment [43], antitumor agent [44,45], and immunomodulator [46] motivated us to

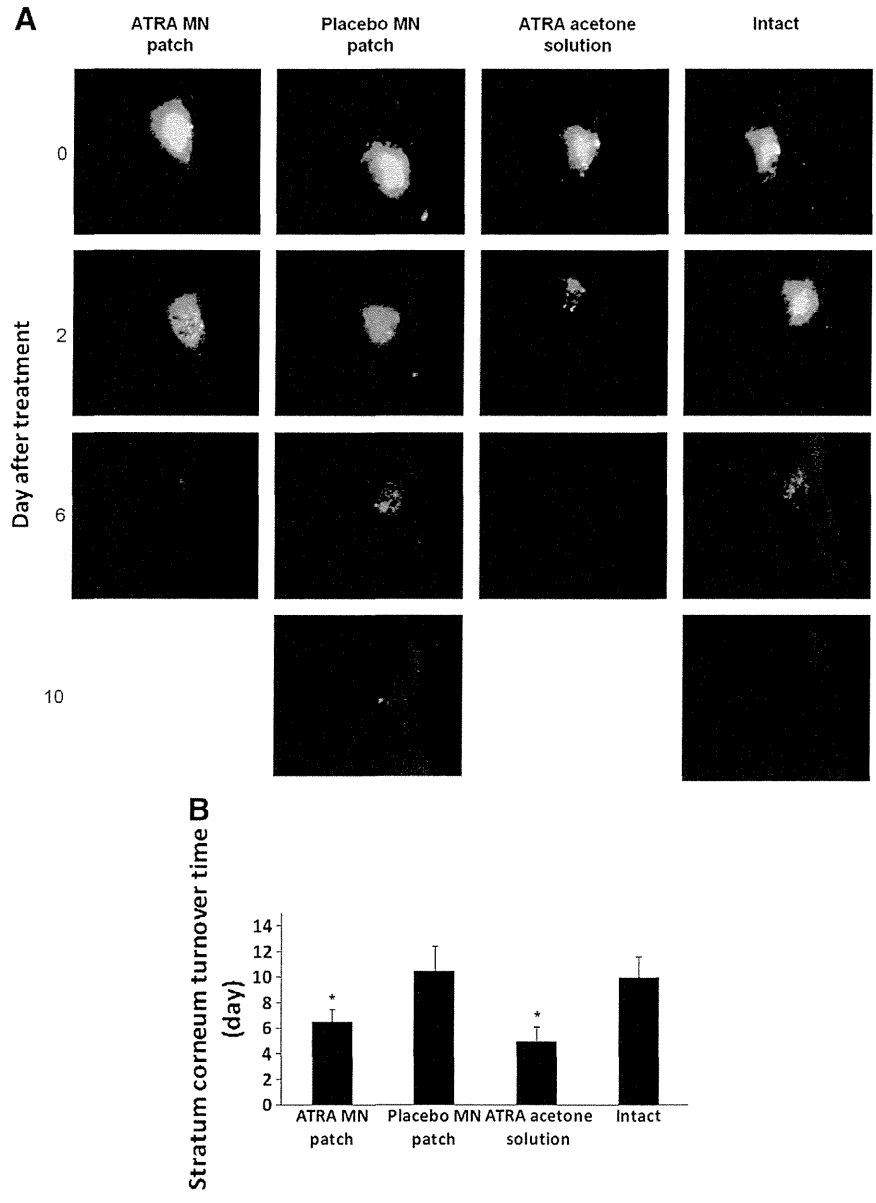

Fig. 4. SCT time assessed by the dansyl chloride method after a single treatment with ATRA-loaded MN patches, placebo MN patches, or ATRA acetone solution. (A) Representative *in vivo* fluorescence imaging for dansyl chloride staining (green spot) from four mice for each group. Images were captured by CRi Maestro EX at the indicated time point after administration. (B) SCT time was expressed as the time in days from administration until the disappearance of the fluorescence corresponding to dansyl chloride staining. Data represent the average ± SD of four measurements. $^*p < 0.05$ vs. intact.

develop an ATRA-loaded MN patch. In our earlier study, we evaluated the performance and characteristics of the ATRA-loaded MN patch, which exhibited good stability and facilitated transcutaneous ATRA delivery into the skin [22]. This achievement allowed us to extend MN technology to therapeutic development in dermatology. Thus, we hypothesized that ATRA delivery to the keratinocyte layer using MN patches will be a novel therapeutic approach to accelerate SCT for SK treatment.

This study evaluated the efficacy of ATRA-loaded MN patches as a simple, alternative therapeutic option to traditional surgical treatments. We first evaluated epidermal hyperplasia using HE-stained skin sections, which demonstrated that the ATRA-loaded MN patches markedly induced epidermal hyperplasia that corresponded to increases in both epidermal thickness and the number of keratinocyte layers. Epidermal hyperplasia was also induced by placebo MN application, but this finding was not unexpected because disruption of the stratum corneum induces epidermal hyperplasia during wound healing in mice [47]. We assumed that creating micron-scale holes while applying MNs and their repair emulated the wound healing process.

Schwartz et al. reported that topical ATRA application stimulates collagen synthesis in the dermis [48]. To further evaluate ATRA activity after ATRA-loaded MN patch application, collagen synthesis was examined by EVG staining. Fig. 1F–J and M demonstrates that the ATRA-loaded MN patch stimulated collagen synthesis in the dermis although the number of skin sections evaluated are only six from each treatment group with semi-quantitative method of visual inspection. This is also supported by a previous report. Microneedling using DermaRoller®, a commercially available cosmetic device, leads to the release of growth factors that stimulate the formation of new collagen and elastin in the dermis [49]. The results of histological evaluation using HE- and EVG-stained skin sections suggest that our ATRA-loaded MN patch can induce epidermal hyperplasia and potential collagen synthesis in the epidermis and dermis, respectively. These findings may potentially lead to further exploration of this new technology for other dermatological areas such as photo-damaged skin.

Topical application of ATRA induces HB-EGF expression in suprabasal keratinocytes in mice [14,15]. We also found that marked HB-EGF mRNA

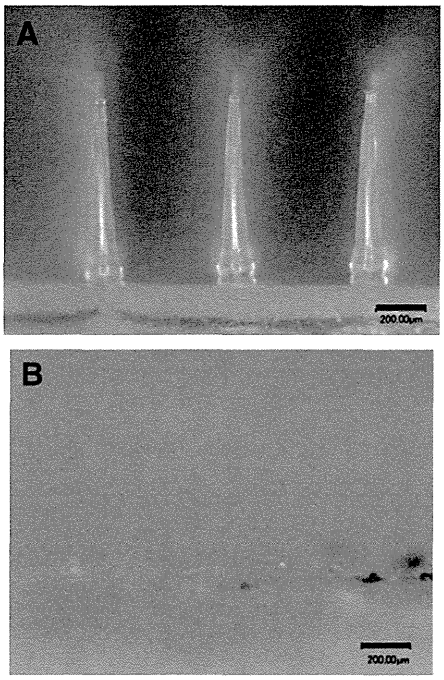

Fig. 5. MN before and after insertion into human skin. Representative photographs of (A) MN patch before application (B) MN patch after application. MN dissolved without MN remaining on the base material. Scale bar, 200 μm.

expression was induced by the ATRA-loaded MN patch. Furthermore, the activity of ATRA in the skin was confirmed by a CRABPII mRNA expression assay. CRABPII is a protein that binds ATRA, modulates its intracellular concentration, and delivers it to appropriate targets [50], and this protein is selectively expressed in normal human and mice skin. Unlike the nuclear retinoic acid receptors, CRABPII expression is markedly increased after topical ATRA treatment. CRABPII mRNA can be used as a reliable and selective marker for ATRA activity in the skin [42]. The data revealed a significant upregulation of CRABPII mRNA after ATRA-loaded MN patch application compared with the effects of placebo MN patch application. The result of fluorescent immunohistochemical staining also confirmed HB-EGF protein induction by the ATRA-loaded MN patch. Thus, these results support that ATRA activity was elicited in the epidermis and dermis, indicating the effectiveness of ATRA-loaded MN patches in mice.

Our therapeutic strategy for SK was to accelerate SCT, resulting in SK lesions falling from the surface of the skin, by facilitating ATRA delivery into the skin using MN patches, which is expected to promote the proliferation of basal keratinocytes. The results of SCT time estimation using dansyl chloride revealed that ATRA-loaded MN patches could successfully accelerate SCT.

Despite their beneficial treatment effects, the topical application of retinoids often results in severe local irritation such as mild erythema and stratum corneum peeling. The erythematous reaction is clinically similar to a form of mild irritant dermatitis called retinoid dermatitis [11,51,52]. However, it is uncertain how topical retinoids induce retinoid dermatitis [11,53]. Our *in vivo* irritation study demonstrated that very slight erythema was caused by ATRA-loaded or placebo MN patch application, whereas ATRA acetone solution caused moderate to severe erythema (Fig. 3A and B). Keratinocytes, which comprise 95% of the cells in the epidermis, provide a reservoir for primary cytokines such as IL-1α, IL-1β, and TNF-α. However, in response to exogenous stimuli, activated keratinocytes can produce inflammatory cytokines such as IL-6, which can be induced by IL-1 and/or TNF-α [54–56]. The biological activity of IL-1α has been identified in keratinocyte cultures, but IL-1α is stored inside cells and is not actively secreted. In contrast, monocytes produce and secrete IL-1β, TNF-α, and IL-6 very effectively in response to exogenous stimuli [57,58]. Thus, to better understand the cause of erythema, we evaluated IL-1β, TNF-α, and IL-6 expression (Fig. 3C–E). IL-1β mRNA expression displayed the highest fold induction in response to ATRA-loaded MN patch application irrespective of the degree of erythema. TNF-α mRNA expression displayed a similar trend as that of IL-1β. As previously reported, impairment of the skin barrier by repeated tape stripping in mice increased epidermal IL-1β and TNF-α

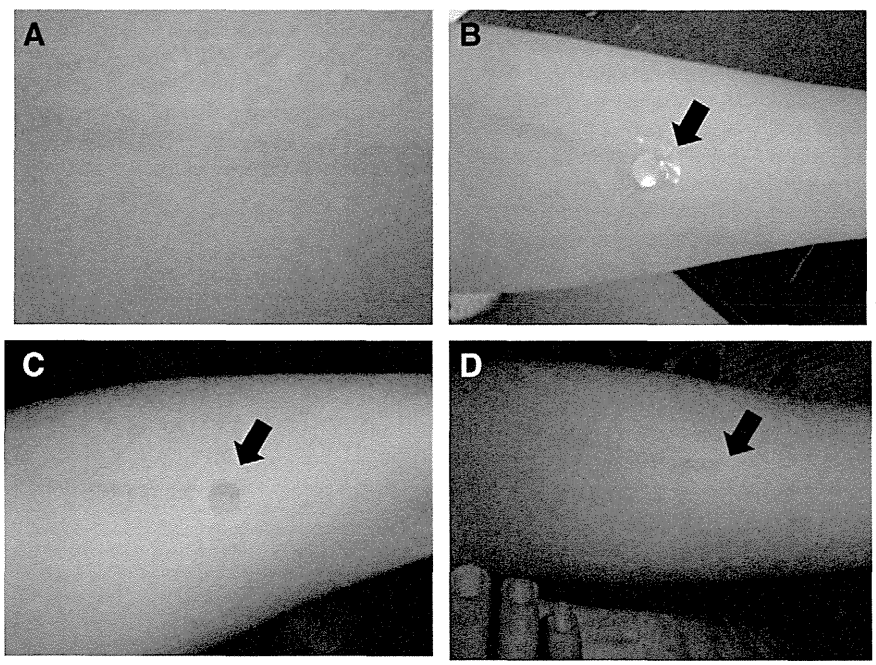

Fig. 6. Safety study in humans. Representative photographs (A) before the application of ATRA-loaded MN patches, (B) after the MN patch was pressed into the skin and left in place for 6 h, (C) 1 day after application (weak positive reaction indicating erythema observed), and (D) seven days after application (negative reaction). Black arrows denote the application site.

Table 1
Assessment of local adverse events in the human safety study.

Subject	Sex	Age	Application site	ICDRG score[a]			Blood tests[b]
				Day 1	Day 7	Day 30	
1	Male	36	Forearm	(+)	(−)	(−)	N.A.C.[c]
2	Female	51	Crus	(?+)	(?+)	(−)	N.A.C.[c]
3	Male	41	Crus	(?+)	(−)	(−)	N.A.C.[c]
4	Female	60	Dorsum manus	(+)	(−)	(−)	N.A.C.[c]

[a] The ICDRG score is denoted as follows:
(−)Negative reaction.
(?+)Doubtful reaction (faint erythema only).
(+)Weak (nonvesicular) positive reaction (erythema, infiltration, and possibly papules).
(++)Strong (vesicular) positive reaction (erythema, infiltration, papules, vesicles).
[b] General blood and biochemical tests of liver and renal function were performed to evaluate the presence of systemic adverse reactions both before ATRA-loaded MN patch application and 48 h after application.
[c] N.A.C.: No abnormal change at 48 h after application compared to the findings before application.

mRNA expression but not IL-6 mRNA expression [56,59]. IL-1β and TNF-α mRNA induction by the ATRA-loaded MN patch may not be dominated by retinoid dermatitis, but this induction may be related to stratum corneum disruption by MNs. The results for IL-6 mRNA expression appear to be consistent with the degree of erythema. However, there was no significant difference in IL-6 mRNA expression among the three groups evaluated (ANOVA, $p > 0.05$), and thus, no clear relation between IL-6 mRNA expression and retinoid dermatitis was demonstrated in this study. Although the degree of erythema was mild, the data indicate that ATRA-loaded MN patch application results in skin irritation in mice.

The safety of ATRA-loaded MN patches with single dosing was assessed in humans. One day after application, a weak positive reaction indicating erythema was observed in human volunteers, in line with the findings of the irritation study in mice. However, seven days after application, almost no reaction was observed. In addition, patch application did not cause systemic adverse effects. Of importance, our developed ATRA-loaded MN patch did not result in serious untoward complications in humans, although the number of subjects was limited with four subjects. These results motivate us to move forward in further exploring the efficacy of these patches against SK in humans.

Our intention of developing ATRA-loaded MN patch is to provide an effective means of ATRA delivery into the skin for a novel therapeutic option. There have been several papers reported thus far using topical application of retinoid for SK treatment; however, complete remissions have not been achieved [9,10]. This may relate to low skin permeability of ATRA. When ATRA gel (commercial formulation of Retin-A 0.025%) was applied to human skin, only 5.5% and 0.44% of ATRA were penetrated into epidermis and dermis, respectively 24 h after application [60], whereas the ATRA-loaded MN patch showed more than 90% delivery rate in mouse in our recent study [22]. Although effective dose for SK has been unknown, ATRA-loaded MN patch can offer flexible dose control by changing loading amount. This is one of advantages over topical formulations because available dose into the skin is limited by the skin penetration ratio of topical formulation. The effective dose and frequency of application in human will be evaluated in future efficacy study after additional safety study of dose rising and multiple repeated dosing.

The size of our fabricated ATRA-loaded MN patch is 0.8 cm^2, which is designed for intended use of self administration for a few small lesions. SK occasionally develops anywhere on the skin excluding the palms and soles with a lot of lesions. Application of 25–50 individual patches may be technically feasible, but not preferable for patients' compliance. In this case, the ATRA-loaded MN patch would benefit patients that are treated unsuccessfully by the standard treatment of cryosurgery, which means ATRA-loaded MN patches are applied to remained lesions. Application with a much larger patch for larger area of lesions may be technically impractical for the point of precise needle insertion into skin. Roller type of MN patch may have a possibility, but our fabrication technology has not been sufficient. This is one of the limitations to overcome considering commercial use of ATRA-loaded MN patch for any types of lesions.

5. Conclusion

This study provides a proof of principle of the feasibility of a dissolving MN patch to administer ATRA without any serious complication in four volunteers. The activity of ATRA was also confirmed in mice by assessing epidermal hyperplasia and HB-EGF and CRABPII mRNA expression, and fluorescent immunohistochemical staining of skin sections revealed the induction of HB-EGF protein. Furthermore, our ATRA-loaded MN patch can accelerate SCT. Overall, we conclude that MN patches can offer an effective means of ATRA delivery into the skin, thus potentially representing an effective pharmaceutical product providing a novel therapeutic option for SK.

Acknowledgments

We acknowledge Kazuyuki Niki and Tomomi Sato at Osaka University for their help with the animal studies. This work was supported by the Advanced Research for Medical Products Mining Programme of the National Institute of Biomedical Innovation (NIBIO); Health and Labour Sciences Research Grants in Research on New Drug Development from the Ministry of Health, Labour, and Welfare; and a Grant-in-Aid for Scientific Research (B) (24390041 and 25293038) from the Ministry of Education, Culture, Sports, Science, and Technology of Japan.

References

[1] J.M. Yeatman, M. Kilkenny, R. Marks, The prevalence of seborrhoeic keratoses in an Australian population: does exposure to sunlight play a part in their frequency? Br. J. Dermatol. 137 (1997) 411–414.
[2] O.S. Kwon, E.J. Hwang, J.H. Bae, H.E. Park, J.C. Lee, J.I. Youn, J.H. Chung, Seborrheic keratosis in the Korean males: causative role of sunlight, Photodermatol. Photoimmunol. Photomed. 19 (2003) 73–80.
[3] C. Hafner, A. Hartmann, F.X. Real, F. Hofstaedter, M. Landthaler, T. Vogt, Spectrum of FGFR3 mutations in multiple intraindividual seborrheic keratoses, J. Invest. Dermatol. 127 (2007) 1883–1885.
[4] C. Hafner, T. Vogt, Seborrheic keratosis, J. Dtsch. Dermatol. Ges. 6 (2008) 664–677.
[5] M. Ming, C.R. Shea, L. Feng, K. Soltani, Y.-Y. He, UVA induces lesions resembling seborrheic keratoses in mice with keratinocyte-specific PTEN downregulation, J. Invest. Dermatol. 131 (2011) 1583–1586.
[6] D. Mehrabi, R.T. Brodell, Use of the alexandrite laser for treatment of seborrheic keratoses, Dermatol. Surg. 28 (2002) 437–439.
[7] S.W. Stoll, J.T. Elder, Retinoid regulation of heparin-binding EGF-like growth factor gene expression in human keratinocytes and skin, Exp. Dermatol. 7 (1998) 391–397.
[8] M.B. Spom, A.B. Roberts, Role of retinoids in differentiation and carcinogenesis, Cancer Res. 43 (1983) 3034–3040.
[9] M.D. Herron, A.R. Bowen, G.G. Krueger, Seborrheic keratoses: a study comparing the standard cryosurgery with topical calcipotriene, topical tazarotene, and topical imiquimod, Int. J. Dermatol. 43 (2004) 300–302.

[10] N.N. Pravit Asawanonda, Porntip Huiprasert, Seborrheic keratosis-like porokeratosis: a case report, Dermatol. Online J. 11 (2005) 18.
[11] G.J. Fisher, J.J. Voorhees, Molecular mechanisms of retinoid actions in skin, FASEB J. 10 (1996) 1002–1013.
[12] J. Varani, M. Zeigler, M.K. Dame, S. Kang, G.J. Fisher, J.J. Voorhees, S.W. Stoll, J.T. Elder, Heparin-binding epidermal-growth-factor-like growth factor activation of keratinocyte ErbB receptors mediates epidermal hyperplasia, a prominent side-effect of retinoid therapy, J. Invest. Dermatol. 117 (2001) 1335–1341.
[13] S. Barrientos, O. Stojadinovic, M.S. Golinko, H. Brem, M. Tomic-Canic, Growth factors and cytokines in wound healing, Wound Repair Regen. 16 (2008) 585–601.
[14] J.-H. Xiao, X. Feng, W. Di, Z.-H. Peng, L.-A. Li, P. Chambon, J.J. Voorhees, Identification of heparin-binding EGF-like growth factor as a target in intercellular regulation of epidermal basal cell growth by suprabasal retinoic acid receptors, EMBO J. 18 (1999) 1539–1548.
[15] B. Chapellier, M. Mark, N. Messaddeq, C. Calleja, X. Warot, J. Brocard, C. Gerard, M. Li, D. Metzger, N.B. Ghyselinck, P. Chambon, Physiological and retinoid-induced proliferations of epidermis basal keratinocytes are differently controlled, EMBO J. 21 (2002) 3402–3413.
[16] L. Rittie, J. Varani, S. Kang, J.J. Voorhees, G.J. Fisher, Retinoid-induced epidermal hyperplasia is mediated by epidermal growth factor receptor activation via specific induction of its ligands heparin-binding EGF and amphiregulin in human skin *in vivo*, J. Invest. Dermatol. 126 (2006) 732–739.
[17] K. Yoshimura, G. Uchida, M. Okazaki, Y. Kitano, K. Harii, Differential expression of heparin-binding EGF-like growth factor (HB-EGF) mRNA in normal human keratinocytes induced by a variety of natural and synthetic retinoids, Exp. Dermatol. 12 (Suppl. 2) (2003) 28–34.
[18] P.A. Lehman, J.T. Slattery, T.J. Franz, Percutaneous absorption of retinoids: influence of vehicle, light exposure, and dose, J. Invest. Dermatol. 91 (1988) 56–61.
[19] S.-J. Lim, M.-K. Lee, C.-K. Kim, Altered chemical and biological activities of all-trans retinoic acid incorporated in solid lipid nanoparticle powders, J. Control. Release 100 (2004) 53–61.
[20] M.G. Brisaert, I. Everaerts, J.A. Plaizier-Vercammen, Chemical stability of tretinoin in dermatological preparations, Pharm. Acta Helv. 70 (1995) 161–166.
[21] C. Sinico, M. Manconi, M. Peppi, F. Lai, D. Valenti, A.M. Fadda, Liposomes as carriers for dermal delivery of tretinoin: *in vitro* evaluation of drug permeation and vesicle–skin interaction, J. Control. Release 103 (2005) 123–136.
[22] Y. Hiraishi, T. Nakagawa, Y.-S. Quan, F. Kamiyama, S. Hirobe, N. Okada, S. Nakagawa, Performance and characteristics evaluation of a sodium hyaluronate-based microneedle patch for a transcutaneous drug delivery system, Int. J. Pharm. 441 (2013) 570–579.
[23] Y.-C. Kim, J.-H. Park, M.R. Prausnitz, Microneedles for drug and vaccine delivery, Adv. Drug Deliv. Rev. 64 (2012) 1547–1568.
[24] A.K. Andrianov, D.P. DeCollibus, H.A. Gillis, H.H. Kha, A. Marin, M.R. Prausnitz, L.A. Babiuk, H. Townsend, G. Mutwiri, Poly[di(carboxylatophenoxy)phosphazene] is a potent adjuvant for intradermal immunization, Proc. Natl. Acad. Sci. U. S. A. 106 (2009) 18936–18941.
[25] Q.Y. Zhu, V.G. Zarnitsyn, L. Ye, Z.Y. Wen, Y.L. Gao, L. Pan, I. Skountzou, H.S. Gill, M.R. Prausnitz, C.L. Yang, R.W. Compans, Immunization by vaccine-coated microneedle arrays protects against lethal influenza virus challenge, Proc. Natl. Acad. Sci. U. S. A. 106 (2009) 7968–7973.
[26] F.S. Quan, Y.C. Kim, R.W. Compans, M.R. Prausnitz, S.M. Kang, Dose sparing enabled by skin immunization with influenza virus-like particle vaccine using microneedles, J. Control. Release 147 (2010) 326–332.
[27] Y. Hiraishi, S. Nandakumar, S.-O. Choi, J.W. Lee, Y.-C. Kim, J.E. Posey, S.B. Sable, M.R. Prausnitz, Bacillus Calmette-Guérin vaccination using a microneedle patch, Vaccine 29 (2011) 2626–2636.
[28] C. Edens, M.L. Collins, J. Ayers, P.A. Rota, M.R. Prausnitz, Measles vaccination using a microneedle patch, Vaccine (2012), http://dx.doi.org/10.1016/j.vaccine.2012.1009.1062.
[29] D.V. McAllister, P.M. Wang, S.P. Davis, J.H. Park, P.J. Canatella, M.G. Allen, M.R. Prausnitz, Microfabricated needles for transdermal delivery of macromolecules and nanoparticles: fabrication methods and transport studies, Proc. Natl. Acad. Sci. U. S. A. 100 (2003) 13755–13760.
[30] J.W. Lee, J.H. Park, M.R. Prausnitz, Dissolving microneedles for transdermal drug delivery, Biomaterials 29 (2008) 2113–2124.
[31] S.P. Sullivan, D.G. Koutsonanos, M. Del Pilar Martin, J.W. Lee, V. Zarnitsyn, S.O. Choi, N. Murthy, R.W. Compans, I. Skountzou, M.R. Prausnitz, Dissolving polymer microneedle patches for influenza vaccination, Nat. Med. 16 (2010) 915–920.
[32] K. Matsuo, S. Hirobe, Y. Yokota, Y. Ayabe, M. Seto, Y.-S. Quan, F. Kamiyama, T. Tougan, T. Horii, Y. Mukai, N. Okada, S. Nakagawa, Transcutaneous immunization using a dissolving microneedle array protects against tetanus, diphtheria, malaria, and influenza, J. Control. Release 160 (2012) 495–501.
[33] K. Matsuo, Y. Yokota, Y. Zhai, Y.-S. Quan, F. Kamiyama, Y. Mukai, N. Okada, S. Nakagawa, A low-invasive and effective transcutaneous immunization system using a novel dissolving microneedle array for soluble and particulate antigens, J. Control. Release 161 (2012) 10–17.
[34] B.M. Tashtoush, E.L. Jacobson, M.K. Jacobson, A rapid HPLC method for simultaneous determination of tretinoin and isotretinoin in dermatological formulations, J. Pharm. Biomed. Anal. 43 (2007) 859–864.
[35] C.C. Willhite, R.P. Sharma, P.V. Allen, D.L. Berry, Percutaneous retinoid absorption and embryotoxicity, J. Invest. Dermatol. 95 (1990) 523–529.
[36] K.J. Livak, T.D. Schmittgen, Analysis of relative gene expression data using real-time quantitative PCR and the 2(−Delta Delta C(T)) Method, Methods 25 (2001) 402–408.
[37] J.H. Draize, G. Woodard, H.O. Calvery, Methods for the study of irritation and toxicity of substances applied topically to the skin and mucous membranes, J. Pharmacol. Exp. Ther. 82 (1944) 377–390.
[38] R. Marks, D. Black, I. Hamami, A. Caunt, R.J. Marshall, A simplified method for measurement of desquamation using dansyl chloride fluorescence, Br. J. Dermatol. 111 (1984) 265–270.
[39] M. Takahashi, D. Black, B. Hughes, R. Marks, Exploration of a quantitative dansyl chloride technique for measurement of the rate of desquamation, Clin. Exp. Dermatol. 12 (1987) 246–249.
[40] U. Ivens, J. Serup, K. O'Goshi, Allergy patch test reading from photographic images: disagreement on ICDRG grading but agreement on simplified tripartite reading, Skin Res. Technol. 13 (2007) 110–113.
[41] Y. Shirakata, R. Kimura, D. Nanba, R. Iwamoto, S. Tokumaru, C. Morimoto, K. Yokota, M. Nakamura, K. Sayama, E. Mekada, S. Higashiyama, K. Hashimoto, Heparin-binding EGF-like growth factor accelerates keratinocyte migration and skin wound healing, J. Cell Sci. 118 (2005) 2363–2370.
[42] J.T. Elder, M.A. Cromie, C.E.M. Griffiths, P. Chambon, J.J. Voorhees, Stimulus-selective induction of CRABP-II mRNA: a marker for retinoic acid action in human skin, J. Invest. Dermatol. 100 (1993) 356–359.
[43] R. Darlenski, C. Surber, J.W. Fluhr, Topical retinoids in the management of photodamaged skin: from theory to evidence-based practical approach, Br. J. Dermatol. 163 (2010) 1157–1165.
[44] B. Ozpolat, G. Lopez-Berestein, Liposomal-all-trans-retinoic acid in treatment of acute promyelocytic leukemia, Leuk. Lymphoma 43 (2002) 933–941.
[45] G. Zuccari, R. Carosio, A. Fini, P.G. Montaldo, I. Orienti, Modified polyvinylalcohol for encapsulation of all-trans-retinoic acid in polymeric micelles, J. Control. Release 103 (2005) 369–380.
[46] I. Skountzou, F.-S. Quan, J. Jacob, R.W. Compans, S.-M. Kang, Transcutaneous immunization with inactivated influenza virus induces protective immune responses, Vaccine 24 (2006) 6110–6119.
[47] M. Denda, K. Kitamura, P.M. Elias, K.K. Feingold, trans-4-(Aminomethyl)cyclohexane Carboxylic Acid (T-AMCHA), an anti-fibrinolytic agent, accelerates barrier recovery and prevents the epidermal hyperplasia induced by epidermal injury in hairless mice and humans, J. Invest. Dermatol. 109 (1997) 84–90.
[48] E. Schwartz, F.A. Cruickshank, J.A. Mezick, L.H. Kligman, Topical all-trans retinoic acid stimulates collagen synthesis *in vivo*, J. Invest. Dermatol. 96 (1991) 975–978.
[49] S. Doddaballapur, Microneedling with DermaRoller, J. Cutan. Aesthet. Surg. 2 (2009) 110–111.
[50] J.L. Napoli, Interactions of retinoid binding proteins and enzymes in retinoid metabolism, Biochim. Biophys. Acta 1440 (1999) 139–162.
[51] B.-H. Kim, Y.-S. Lee, K.-S. Kang, The mechanism of retinol-induced irritation and its application to anti-irritant development, Toxicol. Lett. 146 (2003) 65–73.
[52] S. Kang, E.A. Duell, G.J. Fisher, S.C. Datta, Z.-Q. Wang, A.P. Reddy, A. Tavakkol, J.Y. Yi, C.E.M. Griffiths, J.T. Elder, J.J. Voorhees, Application of retinol to human skin *in vivo* induces epidermal hyperplasia and cellular retinoid binding proteins characteristic of retinoic acid but without measurable retinoic acid levels or irritation, J. Invest. Dermatol. 105 (1995) 549–556.
[53] J.E. Lee, J.Y. Chang, S.E. Lee, M.Y. Kim, J.S. Lee, M.G. Lee, S.-C. Kim, Epidermal hyperplasia and elevated HB-EGF are more prominent in retinoid dermatitis compared with irritant contact dermatitis induced by benzalkonium chloride, Ann. Dermatol. 22 (2010) 290–299.
[54] T.S. Kupper, Immune and inflammatory processes in cutaneous tissues. Mechanisms and speculations, J. Clin. Invest. 86 (1990) 1783–1789.
[55] J.N.W.N. Barker, C.E.M. Griffiths, B.J. Nickoloff, R.S. Mitra, V.M. Dixit, Keratinocytes as initiators of inflammation, Lancet 337 (1991) 211–214.
[56] I. Effendy, H. Löffler, H.I. Maibach, Epidermal cytokines in murine cutaneous irritant responses, J. Appl. Toxicol. 20 (2000) 335–341.
[57] R. Mizutani H Fau -Black, T.S. Black R Fau - Kupper, T.S. Kupper, Human keratinocytes produce but do not process pro-interleukin-1 (IL-1) beta. Different strategies of IL-1 production and processing in monocytes and keratinocytes, J. Clin. Invest. 87 (1991) 1066–1071.
[58] H. Mizutani, Y. Ohmoto, T. Mizutani, M. Murata, M. Shimizu, Role of increased production of monocytes TNF-α, IL-1β and IL-6 in psoriasis: relation to focal infection, disease activity and responses to treatments, J. Dermatol. Sci. 14 (1997) 145–153.
[59] L.C. Wood, S.M. Jackson, P.M. Elias, C. Grunfeld, K.R. Feingold, Cutaneous barrier perturbation stimulates cytokine production in the epidermis of mice, J. Clin. Invest. 90 (1992) 482–487.
[60] M.J. Skov, J.W. Quigley, D.A.W. Bucks, Topical delivery system for tretinoin: research and clinical implications, J. Pharm. Sci. 86 (1997) 1138–1143.